UNIVERSITY OF TURKU

Carbon material effects on Prussian blue solid boosters for flow batteries

Master's Degree Programme in Materials Science
Department of Mechanical and Materials Engineering, Faculty of Technology
Master of Science in Technology Thesis

Author:
Rosa Tirronen

Supervisors:
Dr. Eduardo Martínez González
Professor Pekka Peljo

13.3.2025

The originality of this thesis has been checked in accordance with the University of Turku quality assurance system using the Turnitin Originality Check service.

Master of Science in Technology Thesis
University of Turku

Subject: Materials Science
Author: Rosa Tirronen
Title: Carbon material effects Prussian blue solid boosters for flow batteries
Number of pages: 52 pages
Date: 13.3.2025

High energy density flow batteries (FBs) are critical technologies for the large-scale storage of intermittent energy produced by solar and wind power. Advancing air-stable energy storage posolytes (tanks for storing positive charge) with high volumetric capacity is essential for the development of cost-effective FBs. A promising approach to achieve high volumetric capacity involves charging Prussian blue (PB, which undergoes a $4e^-$ reduction process in water at a relatively high redox potential) solid boosters in external tanks (outside a glove box) using a $[Fe(CN)_6]^{4-/3-}$-based neutral aqueous electrolyte as the charge-transporting solution. However, no formulations for preparing these boosters have been reported, and costly machinery was employed in their preparation. In this thesis, a cost-effective procedure for preparing PB solid boosters was developed, and various formulations of these species were explored by adjusting the percentage of binder, carbon black, KCl and PB (65-70%) in their composition. Four different commercially available carbon materials were used in the formulations, and their effects on the cycling stability and utilisation capacity of the resulting boosters, tested in $[Fe(CN)_6]^{4-/3-}$-based FBs, are discussed. Significant effects of this varied material on both properties were found. The best-performing boosters achieved FB cycling stability (more than 1000 charge-discharge cycles) and utilisation capacity (73.3%) comparable to those reported in the literature. The results also suggest that future reformulation of boosters with the other carbon materials could further advance this emerging technology.

Keywords: aqueous flow batteries, Prussian blue solid boosters, ferri/ferrocyanide, cost-effective synthesis, carbon material effects

Diplomityö
Turun yliopisto

Oppiaine: Materiaalitekniikka
Tekijä: Rosa Tirronen
Otsikko: Hiilimateriaalin vaikutus preussinsininen-partikkeleihin virtausakuissa
Sivumäärä: 52
Päivämäärä: 13.3.2025

Korkean energiatiheyden virtausakut (FB:t, ”flow batteries”) ovat keskeinen teknologia aurinko- ja tuulivoiman tuottaman vaihtelevan energian laajamittaiseen varastointiin. Ilmaolosuhteissa vakaiden, suuren tilavuuskapasiteetin omaavien posolyyttien (säiliö positiiviselle elektrolyytille) edistämiseksi on olennaista kustannustehokkaiden virtausakkujen kehittämisessä. Yksi lupaava tapa korkean tilavuuskapasiteetin saavuttamiseen on preussinsinistä (PB, “Prussian blue”, jolla on neljän elektronin pelkistymisreaktio vedessä verrannaisesti korkeassa redox-potentiaalissa) sisältävien kiinteiden partikkeleiden asettaminen akun säiliöön (hanskakaapin ulkopuolella). Partikkeleiden preussinsininen ladataan käyttämällä neutraalia vesipohjaista ferri-/ferrosyanidielektrolyyttiä varausta kuljettavana liuoksena. Näiden partikkeleiden tarkkaa koostumusta ei ole kuitenkaan raportoitu, ja lisäksi niiden valmistamiseen on käytetty kalliita laitteita. Tässä työssä kehitettiin kustannustehokas menetelmä PB-partikkeleiden valmistamiseen, sekä tutkittiin erilaisia koostumuksia säätelemällä sideaineen, hiilimustan, kaliumkloridin ja PB:n (65-75 %) osuutta. Näissä koostumuksissa käytettiin neljää erilaista kaupallisesti saatavilla olevaa hiilimateriaalia. Työssä selvitettiin hiilimateriaalien vaikutusta lataus-purkaussyklien kestävyyteen ja partikkeleiden hyödyntämiskapasiteettiin ferri-/ferrosyanidivirtausakuissa. Hiilimateriaalin vaihtamisen havaittiin vaikuttavan merkittävästi näihin ominaisuuksiin. Parhaiten toimineet partikkelit saavuttivat virtausakussa yli tuhat lataus-purkaussykliä ja 73.3 prosentin hyödyntämiskapasiteetin, mikä on verrattavissa raportoituihin samankaltaisiin systeemeihin. Tulokset viittaavat myös siihen, että partikkeleiden jatkokehitys muidenkin hiilimateriaalien kanssa voisi entisestään edistää tätä teknologiaa.

Keywords: vesipohjaiset virtausakut, kiinteät sähkönvaraajat, preussinsininen, ferri/ferrosyanidi, hiilimateriaalin vaikutus

Table of contents

Abbreviations

CB	Carbon black
CC	Constant current
CC-CC	Constant current, two steps
CC-CP	Constant current and constant potential
CE	Coulombic efficiency
CE’	Counter electrode
CP	Constant potential/constant voltage
CV	Cyclic voltammetry
FB	Flow battery
EE	Energy efficiency
PB	Prussian blue
PW	Prussian white
RE	Reference electrode
RFB	Redox flow battery
SECM	Scanning electrochemical microscopy
VE	Voltage efficiency
WE	Working electrode

1 Introduction

Integrating solar and wind energy sources into power grids poses a major challenge in the ongoing energy transition [1]. Developing cost-effective electrochemical energy storage devices is essential for achieving successful integration of intermittent sources. A promising approach for large-scale and mid-duration energy storage uses flow batteries (FBs), where posolyte (solution to store positive charge) and negolyte (solution to store negative charge) electrolytes are charged inside an electrochemical cell and pumped to separate external tanks for storage, leading to a decoupling power and energy density [2]. The latter property is often limited by a relatively low solubility of electroactive material. By charging-discharging electricity without experiencing electrolyte degradation, the all-vanadium configuration is the most deployed flow battery (FB) in the market [2], but its further development is restricted to the low energy density, corrosive solvent (2 mol L^{-1} H_2SO_4) and fluctuating price of vanadium [3]. Therefore, it is promising to develop FB electrolytes composed of earth-abundant electroactive materials.

A wide range of alternative materials is available for preparing negolyte electrolytes. Designing posolyte solutions remains challenging due to the limited availability of electroactive materials that have proven effective for positive charge storage, making it promising to focus on improving the performance of the latter systems. In this context, ferricyanide/ferrocyanide ($[Fe(CN)6]^{3-/4-}$) is an earth-abundant and air-stable electroactive material, which exhibits fast and reversible charge transfer kinetics in neutral aqueous solvents. Although it has been extensively considered as electroactive species of posolytes in various FB configurations, its low water-solubility provides storage tanks with low volumetric capacity [4, 5].

Taking advantage of the low cost and corrosiveness of $[Fe(CN)_6]^{3-/4-}$ redox couple, a new tank design for FB posolytes was recently introduced, where Prussian blue (PB) solid boosters are chemically charged-discharged at the storage tank using the former redox couple as charge-transporting species from the electrode surface to the particles, via the pumped solution [3, 6]. In this configuration, the volumetric capacity is relatively high because it primarily relies on the fourth-electron storage capacity of the PB/Prussian white (PW) redox couple, which makes up more than 60 % in the solid boosters. The latter material is also abundant, cost-effective and can be charged-discharged outside a glovebox. Despite these significant advances, improving the performance of solid boosters remains a challenge, as no formulation for their preparation has been reported, and their synthesis requires expensive machinery.

Therefore, in this thesis, it was set out to develop a simple strategy for preparing solid boosters composed of the materials PB, conductive carbon and the binder poly-ethylene-co-acrylic acid (PEAA). The idea was inspired by a previous work developed by our group [7], where a cost-effective procedure for preparing PW solid boosters was reported, but the long-term cycling stability of the resulted boosters remained to be demonstrated, since the author only presented results for FBs operating for less than 41 charge-discharge cell cycles. In this thesis, four different carbon materials were used in the preparation of the boosters to study carbon material effects as well. The results exhibited a significant effect of the type of carbon material on the utilisation capacity of the boosters charged-discharged in symmetric FB cells, utilizing ferricyanide-ferrocyanide solutions as charge-transporting species. The best-performing formulation demonstrated long-term cycling stability (over 1000 charge-discharge cycles) and utilisation capacity (> 70 %), comparable to those reported in the literature for PB solid boosters prepared with sophisticated and expensive equipment. Therefore, in this thesis, effective booster formulations were developed that worked synergistically with ferro-ferri solutions, enhancing the charge storage capacity of aqueous neutral FB posolytes.

2 Ferrocyanide-based flow battery electrolytes

Aqueous FBs can operate at acidic, alkaline and neutral conditions. Neutral batteries enable operation with less corrosive electrolytes [3], and substantial progress has been made in the development of electroactive molecules for preparing neutral electrolytes. Some systems include, but are not limited to, viologens [8], anthraquinones [9] and phenazines [10]. In the case of negolytes, current research is mainly focused on improving the long-term cycling stability and water solubility of electroactive materials, which complicates the development of liquid-solid tanks for the storage of negative charge. In other words, charging boosters with unstable electroactive solutions would not be practical, and the results could be hard to interpret, since it would be difficult to determine whether the booster is not functioning properly and/or if the electrolyte is degrading.

For the posolyte side, there are only few types of electroactive materials prepared for this purpose and most of them also have challenges that must be solved before they can work in synergy with solid boosters in energy storage tanks. Improving the long-term charge-discharge cycling stability of the solutions is also challenging. One promising compound to develop neutral posolytes is 2,2,6,6-Tetramethylpiperidin-1-yl oxyl (TEMPO), but its decomposition mechanism related to battery failure remains unclear, some studies suggest the presence of decomposition products derived from dismutations [11].

Phenoxazines were recently used in the preparation of posolytes for neutral pH applications, but their cycling stability is still under investigation because the batteries degrade in the first charge-discharge cell cycles [12, 13]. Although phenoxazines are highly soluble, the primary challenge remains long-term cycling stability due to rapidly degrading material. Other organic structures have also been proposed to develop neutral electrolytes and work continues to focus on understanding the degradation mechanism of electrolytes to improve the long-term cycling stability of the systems. Therefore, developing solid boosters for the latter cases does not make sense for now.

A wide variety metal complexes (e.g., cobalt-based systems) have also been studied as potential posolyte electroactive materials, but they face similar challenges, including low solubility and poor stability [14]. Another example is 1,1´[3-(trimethylammonio)propyl]ferrocene dichloride, which has demonstrated excellent stability as a posolyte in aqueous neutral conditions [15]. However, despite its promising performance, the challenge here is that it’s not yet cost-effective

material for large scale energy storage applications, limiting its practicality in commercial flow battery systems.

Finally, ferri/ferrocyanide pair has served as a reference material in the study of various negolyte electrolytes, serving as a cost-effective and highly stable posolyte material for neutral and alkaline applications. When compared to the other molecules presented above, this system exhibits good chemical and electrochemical stability, excellent reversibility and fast charge transfer kinetics [16].

The ferri/ferrocyanide pair not only offers the advantage of working in neutral conditions, but is also a low-corrosive material that can undergo reversible electron transfers in the presence of oxygen, which is crucial for developing cost-effective and flexible applications. In other words, this electrolyte can operate in FBs outside a glovebox. additionally, iron is the second most abundant metal in the Earth's crust, making it a readily available and sustainable material.

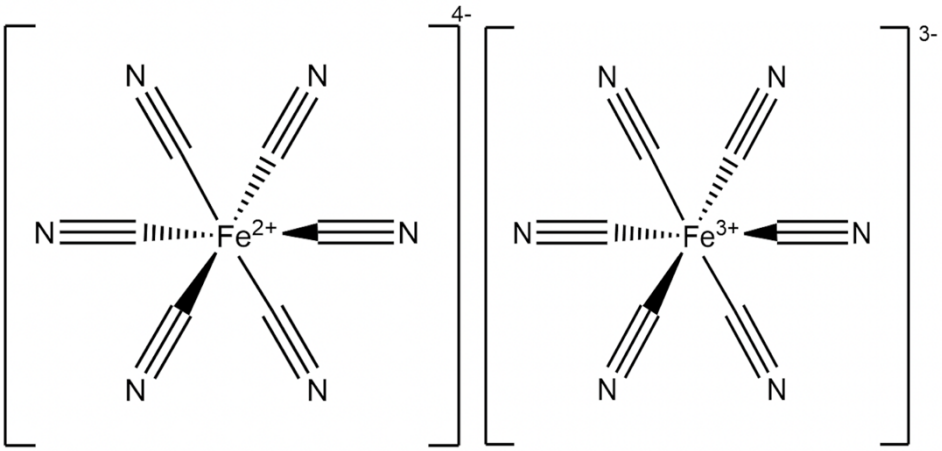

Figure 1: Chemical structure of ferrocyanide (left) and ferricyanide (right) molecules

Another significant benefit of ferri/ferrocyanide couple is its wide flexibility in pairing with various negolytes, including organic ones (and can be applied also in alkaline conditions) [6]. When utilizing this electrolyte, the electron transfer process occurring at the electrode material is described as follows [3], where one-electron is transferring per molecule:

$$Fe(CN)_6^{3-} + e^- \rightleftharpoons Fe(CN)_6^{4-} \quad (1)$$

Despite these advantages commented above, ferri/ferrocyanide pair is a promising material limited by its moderate solubility, which further limits the volumetric capacity. For example, solubility of the compound is approximately 0.4 mol L^{-1} in KCl [16]. Its low volumetric capacity is also due to its redox process involving only a single-electron transfer per molecule.

A common strategy to improve the solubility of electroactive materials is by introducing substituent groups into the moleculess, which works well for organic systems. However, this strategy does not apply to metals. Instead of this, complexing agents or solubilizing ligans are commonly used [14]. However, modulating the chemical structure of ferri-/ferrocyanide molecules with complexing agents has not been promising. So, cyanide species remain critical to provide moderate solubility in this system [17].

Mixing sodium and potassium counterions is another promising approach to improve the water-solubility of ferri-/ferrocyanide molecules. Exceptional results were demonstrated by improving the solubility up to 1.5 M [6]. This improved electrolyte can perform efficiently against negolytes that transfer one-electron per molecule, or against systems that store two-electrons per molecule but have significantly lower solubility. But work is required on the development of high volumetric capacity and systems undergoing two-electrons per molecule are important.

There are already systems of two-electron storage capacity and for them, the ferri-/ferrocyanide electrolyte, even with its relatively high solubility in the presence of K^+ and Na^+ counterions, often limits the design of compact storage tanks [3, 18], which is not practical for real-world applications. Additionally, in some cases, even for molecules of one-electron storage capacity, this counterion strategy may not be ideal, as certain counterions can travel through the membrane, leading to undesired effects with some materials. In some cases, the negolyte electroactive material is unstable in the presence of either potassium or sodium, resulting in the formation of large precipitating aggregates. For instance, Gallocyanine compound is soluble KOH solutions but precipitate in the presence of Na^+ counterions [19].

Therefore, with the aim to design more compact systems, it is promising to work on alternative strategies to improve the charge storage capacity of aqueous neutral ferri/ferrocyanide-based posolytes.

3 Solid boosters for ferri/ferro-based posolytes

An alternative strategy for designing compact tanks of high volumetric energy storage capacity involves charging Prussian blue solid boosters in tanks utilising ferri-/ferrocyanide solutions as charge-transporting intermediates. In this configuration, Prussian blue (PB) is an additional electroactive material with low water-solubility (less than 0.1 mMol L^{-1}) that can receive 4 electrons per molecule in a same thermodynamic condition, exhibiting a reversible redox reaction, as described in equation 2 [3]:

$$4K^+ + Fe_4^{3+}[Fe^{2+}(CN)_6]_3 + 4e^- \rightleftharpoons K_4Fe_4^{2+}[Fe^{2+}(CN)_6]_3 \quad (2)$$

PB solid particles can be prepared by mixing this material with carbon conductive materials and a binder [7]. The latter two components are only marginally affecting the chemical and redox properties of the Prussian blue/Prussian white redox couple [7, 20]. Therefore, the modified material can be placed in the tank(s) of the battery to store charge to solid state form, enhancing the performance of the posolyte. Note that PB undergoes a reduction process, which would apparently indicate its use in the development of negolytes. Due to its relatively high redox potential, its reduction product (PW) is the interesting species that can be used for developing posolytes.

The main advantage of working with solid boosters is that the volumetric capacity is no longer determined by the relatively low solubility of the ferri-/ferrocyanide electroactive material, since the molecules work in this configuration as charge-transporting species from the electrode inside the cell, traveling through pipes, to the surface of the boosters to chemically charge-discharge them [21]. The coupling both electroactive materials is possible because both electroactive materials have quite similar redox potential in aqueous electrolytes, allowing them to be effectively charged-discharged inside a battery.

During the charging process of PB solid boosters in symmetric cells, Fe^{3+}-ions in the negolyte tank are reduced to Fe^{2+}-ions by receiving electrons from the electrode placed at the negolyte side. The opposite reaction happens at the posolyte tank that does not contain boosters. The Fe^{2+}-ions produced within the cell at the negolyte site then travel through pipes and begin to accumulate in storage tanks until the driving force is sufficiently to begin charging the boosters, where PB is chemically reduced to PW. In this process, the Fe^{2+}-ions are simultaneously oxidized back to Fe^{3+}-ions, which then travel back to the cell and repeat the process. Note that the concentration of the electroactive species in solution is also important, since four active

molecules are needed to completely charge-discharge each molecule of PB. The global operation of the symmetric cell is represented in Figure 2.

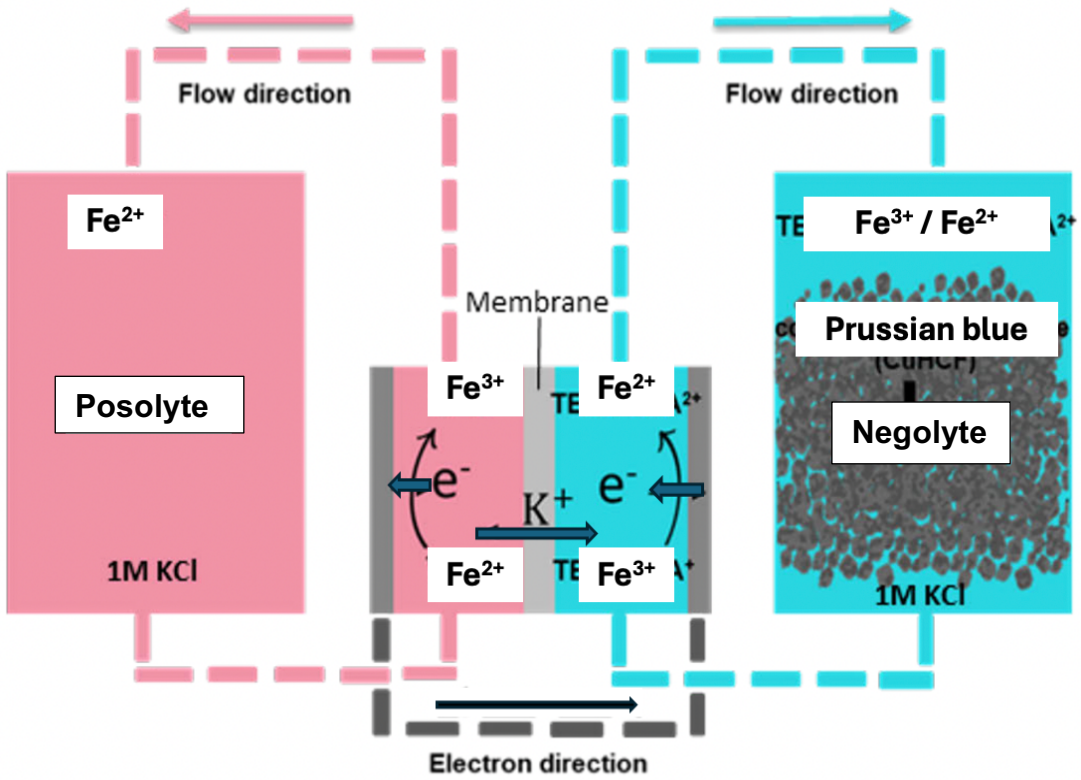

Figure 2: Schematic of a symmetric flow battery consisting of a single electrochemical cell, two energy storage tanks, cation exchange membrane, ferri/ferrocyanide pair in KCl as an electrolyte and solid boosters in the negolyte tank. Edited from thesis by Moghaddam [21]

The graphical representation does not include the intercalation phenomenon of the systems that occurs when charging-discharging the cell, but basically refers the process by which, counter ions must interact with the solid boosters to compensate for the negative charge upon operating the system to ensure charge neutrality within the bulk material [21]. Therefore, the kinetics of the electron transfer process are depending on the size of the counter ions. Smaller species, such as sodium (Na^+) can diffuse faster through the solid booster than larger counter ions like potassium (K^+). Although, counterions can exert a significant impact on the performance of the cell, this kinetic analysis continues to be challenging.

Promising results of the employment of PB solid boosters in ferri-/ferrocyanide-based tanks were reported recently. For example. Yan et al. demonstrated the development of storage tanks of high volumetric capacity (95.7 Ah L^{-1}) by charging PB solid boosters with ferri-/ferrocyanide charge-transporting solutions [3]. The authors also demonstrated a long-term cycling stability of the system, reporting more than thousand charge/discharge cell cycles. With a similar system,

Chen et al. reported a stable cell operation with at least 500 cycles over 871 hours, achieving a volumetric capacity of 61.6 Ah L^{-1}[6]. The maximum utilisation capacity for energy storage in these solid boosters was reported to be 61.0 % and 73.5 %, respectively.

These studies highlight the potential for further improving the performance of Prussian blue solid boosters for neutral aqueous flow battery applications. Despite the impressive results reported, advancing this concept faces challenges due to the following reasons. While the ability of solid boosters to enhance the volumetric capacity has been demonstrated, there is a lack of information regarding the formulations used to prepare the particles. This information is crucial for advancing the development of PB-based solid boosters in flow battery applications.

Secondly, for the latter studies the authors utilized granulation machines in the booster preparation, which significantly increases production costs [3, 6]. An interesting alternative for preparing cost-effective Prussian blue booster systems was recently introduce in a thesis by Balducci [7]. The author avoided the use of expensive machines to prepare the boosters and, in addition, provided a detailed explanation of the preparation procedure. However, Balducci was aware that the cycling stability of the particles operating in FB cells needs to be improved, as only systems operating for up to 40 charge-discharge cycles were studied. Furthermore, another aspect that needs to be improved is the utilisation capacity, which is crucial for developing systems of high-tank volumetric capacity.

Based on this information, solid boosters can be prepared with Prussian blue as an electroactive material, poly-ethylene-co-acrylic acid (PEAA) as a binder and carbon black as a conductive material. Balducci also reports the specific amount of each material, but modifications to these amounts must be made if the systems need to be optimized. In the case of binder material, PEAA, is also used as a binder in the fabrication of electrodes for Lithium-ion batteries. Similar formulations where reported (80wt.% active material, 12wt% carbon black and 10wt% binder) for systems of good performance [22].

In order to improve the performance of the boosters, the properties of the carbon material can also be modified by choosing carbons of different surface area and porosity. Some easily acquired carbon materials that allow these effects to be studied are YP-50F, YP-80F, BP2000 and C65. All of these materials are commercially available, highly conductive and have high surface area. YP-50F and YP-80F are both coconut-shell activated materials sealed by a company called Kuraray [23]. BP2000 is a very high surface area carbon produced by Cabot.

The latter carbon has been reported to exhibit exceptional electrical conductivity [24, 25]. C65 is a carbon black structure of low surface from Nanografi [26].

Based on this information, it is expected that significant effects of carbon material properties on the performance of PB solid boosters will be detected when charging-discharging FBs. The effects should be capable of being analysed using electrochemical techniques.

4 Electrochemical tools for studying flow batteries

From the above discussion, it is evident that flow batteries work on electrochemical principles, where electron transfer processes take place at electrode materials in separated half cells, upon charging and discharging the cell. As a result, these systems can be analysed by electrochemical techniques. For example, the redox potential of each half cell is an important factor which determines the overall voltage of the cell. Another important parameter is the reversibility of the system, which has an influence on both efficiency and long-term cycling stability. The fundamental principles governing battery operation are typically examined by cyclic voltammetry, and battery performance tests can be performed with polarization techniques.

4.1 Cyclic voltammetry

Reversibility in electrochemical reactions refers to the ability of a redox reaction to happen efficiently in both oxidation and reduction directions, without causing a significant degradation in the performance of the cell. This characteristic is fundamental for repeatedly charging-discharging energy storage systems such as FBs, to achieve minimal loss of efficiency, while maintaining good performance and cycling stability [27].

Reversible reactions allow for faster charge-discharge rates of the electrolytes. Electron transfer reversibility refers to the rate of electron transfer between redox components (charge transfer species) and the electrodes. Reversible reactions have fast electron transfer kinetics and maintain equilibrium at the electrode interface. On the contrary, irreversible systems are defined by slow electron transfer, which can have a significant effect on power output and overall performance of the system. Between these two more extreme cases are quasireversible reactions, displaying moderate electron transfer rates that can be affected by factors like reactant diffusion and properties of electrode surface.

Information on reversibility, electron transfer rate and redox potential, can be analysed with cyclic voltammetry [28]. Cyclic voltammetry (CV) is an electrochemical non-destructive technique to examine oxidation and reduction processes of active materials. It is a potential sweep method, which means measuring the current change as a function of time while changing the potential at constant rate [29]. CV requires a relatively simple setup with a three-electrode system and a potentiostat. A three-electrode system (can be seen in figure 3) has a working electrode (WE), counter electrode (CE') and an aqueous reference electrode (RE), all of them placed in an electrolyte solution. When current is passing between WE and CE', the potential WE with respect to RE is measured [29].

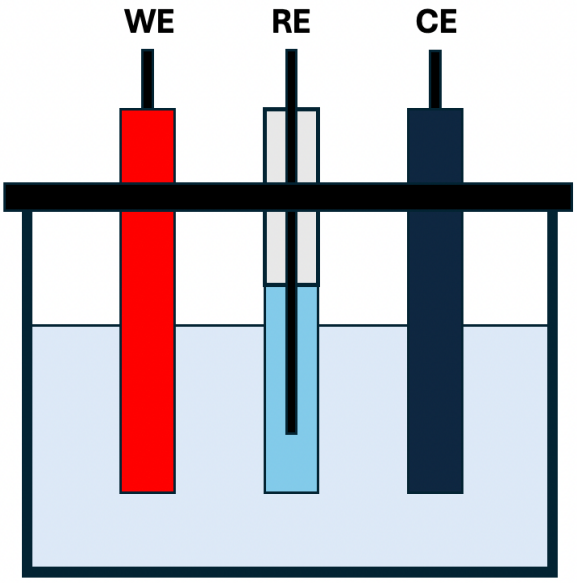

Figure 3: Schematic representation of a three-electrode cell.

Cyclic voltammetry is a powerful tool that can also give visual information on the reversibility of the system through changes in a cyclic voltammogram that includes oxidation and reduction waves or peaks [27].

Well-defined and symmetric oxidation and reduction peaks with minimal separation of the peaks refers to reversible redox couple. In the contrary, broadened and asymmetric peaks with a large separation between the oxidation and reduction peaks reveals an irreversible system. Quasi-reversible systems fall between these two, or in other words, refer to an intermediate region between both latter cases, due to a moderate electron transfer kinetics.

In addition to reversibility, CV enables the quantitative analysis of key electrochemical parameters, such as the diffusion coefficient and the standard rate constant. Both parameters are important in the performance of FBs, especially for electrolytes charging boosters, the redox potential of the charge-transporting solution and solid boosters should be similar. In addition, the diffusion coefficient and electrode kinetics should be in the same order of magnitude as well.

As the redox potentials estimated by CV experiments refers the potential of half cells, the cell voltage of a FB is the result of the potential difference between both half-cells. The electrolyte with the lowest potential is placed at the negative electrode of the battery and is called negolyte. The reverse is true for cathode or posolyte. In the case of symmetric cells, there is no potential

difference or it is 0V, since the battery is assembled with the same redox couple but in different redox states. These symmetric cells are crucial for studying long-term cycling stabilities.

4.2 Polarization technique

Polarization of a battery describes the change in voltage at electrodes due to the flow of current. When charging-discharging a battery, the current and potential variations at the half cells are described by the Butler-Volmer equation [29, 30], both branches are incorporated in the following model:

$$i = i_0(\exp\left[\frac{\alpha_a zF}{RT}(E - E^0)\right] - exp\left[\frac{\alpha_c zF}{RT}(E - E^0)\right]) \ , \tag{3}$$

where E is the electrode potential (in Volts), E^0 is the equilibrium potential (in Volts), α_a and α_c are anodic and cathodic charge transfer coefficients respectively, F is the Faraday constant, R is the molar gas constant, T is the temperature (in Kelvins). For a discharging process of a battery, an experimental profile of the current and the potential as a function of time is typically exhibiting a behaviour presented on figure 4.

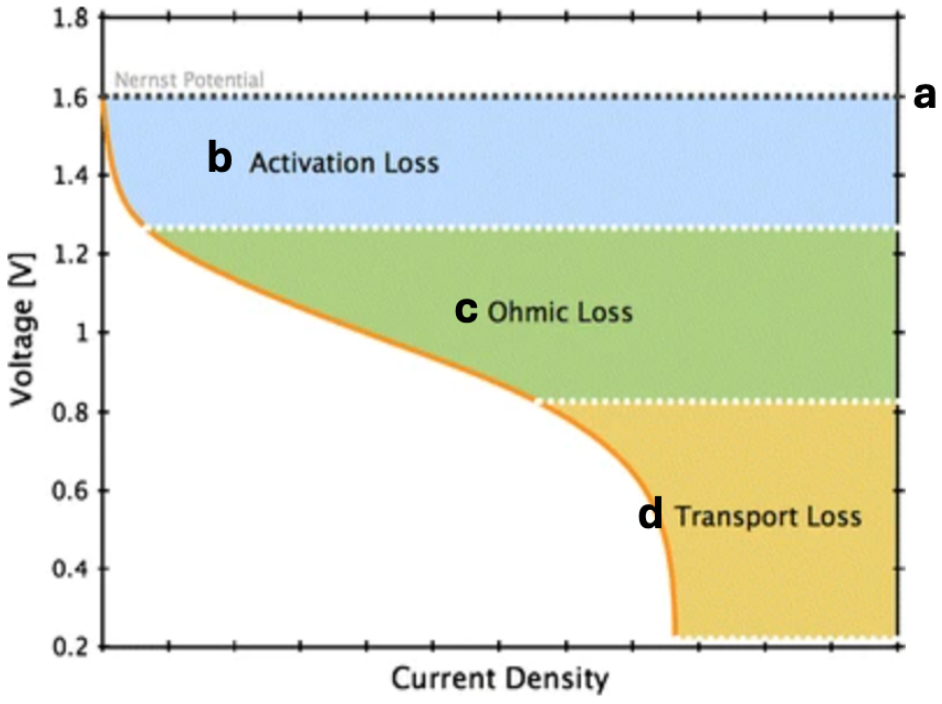

Figure 4: Polarization curve for vanadium flow batteries with representation of losses in charging process, edited from [32]

The charge-discharge process of a battery can be done with a battery cycler. Constant potential (CP) can be applied between the electrodes, observing changes in current as a function of time. This is also dependent on the concentration of electroactive species. Another charging-

discharging process can be done with applying constant current (CC) [31]. With CC the voltage is changing as a function of time and the potential tends to rapidly increase-decrease, when the electroactive material tends to be empty. Therefore, cut-off limits should be placed in both cases to protect the solutions from rapid and sever degradation, for example, due to water oxidation and/or reduction reaction electrolyses.

The theoretical cell potential ($E = E_c - E_a$, Figure 3A) of the cell is determined by the potential difference between both electrolytes given by Nerns't equations below [29]:

$$E_a = {E_a}^0 + \frac{RT}{F}\ln\left(\frac{a_{ox,a}}{a_{red,a}}\right), \text{ negolyte} \quad (4)$$

$$E_c = {E_c}^0 + \frac{RT}{F}\ln\left(\frac{a_{ox,c}}{a_{red,c}}\right), \text{ posolyte,} \quad (5)$$

where E^0 is the standard cell potential (in Volts), R is the molar gas constant, T is the temperature (in Kelvins), F is the Faraday constant, a_{ox} and a_{red} are the activity coefficients for the oxidized and reduced forms of electroactive materials, respectively. The magnitudes are defined for the negolyte (neg) and posolyte (neg) tanks. For practical reasons, the activity coefficients can be replaced by the concentration of species.

Considering a discharging process and applying constant current between the electrodes, in the ideal case, the battery should provide a voltage determined by Nernst equation ($E = E_c - E_a$). However, in reality the battery cannot supply this voltage due to three main sources of potential loss, impacting the performance by reducing the energy efficiency and related parameters. Firstly, the activation losses [32], which refers to activation energy required for electrochemical reactions to take place (at the electrodes) due to the energy barrier that must be overcome for charge transfer to cross the electrode-electrolyte interface. In other words, the kinetics at the electrode is depending on the electronic properties of the material; molecules also waste energy when reorganizing their structures to receive or release the charge, the electrode properties can also be affected by adsorption interactions, and the solvent viscosity can slow down the rate kinetics [33]. Those contributions are typically included by the charge transfer coefficient.

Secondly, Ohmic loss [32], which refers to the resistance to ion flow through the membrane and other cell components upon discharging the cell. It depends on the conductivity across the membrane and cell components and also on the distance between the electrodes. In addition to activation and Ohmic losses, third factor in determining the efficiency of the battery are transport losses. Transport losses are caused by limitations in the movement of charged species

or charge transfers in the electrolyte. For example, if the pumping rate of the electrolyte is too low, some molecules that could otherwise be charged may remain unutilized in the tank. Transport losses depend on the flow rate of electrolyte and also on the diffusion coefficient of electroactive species. For the charging process, the I/E behavior is also similar but in opposite direction. That means, the voltage will start rising upon charging.

When charging with constant potential, the voltage difference between charger and battery determines the charging current [31]. To apply controlled CC and/or CP over defined time periods and analyse our battery's performance through parameters like efficiency and cycle life, we can use a device called battery cycler. Battery cyclers allow us to create a program which specifies whether and how much we are applying CC or CP. The battery goes through charge and discharge cycles when connected to a battery cycler and wanted parameters can be analysed through a computer connected to the cycler.

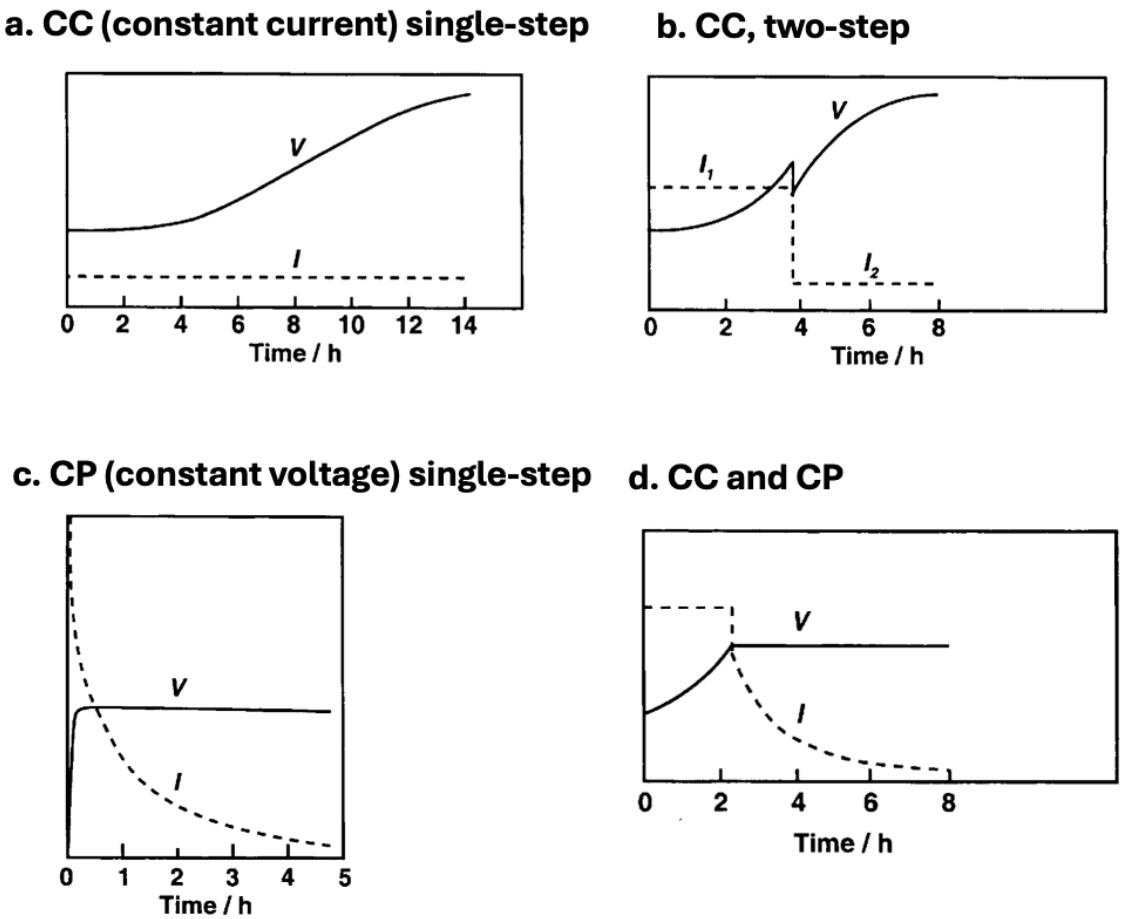

Figure 5: Procedures for charging batteries, edited from [31]

When charging with constant current the current remains steady and voltage is changing as the function of time (figure 5a). Charging with constant current allows for straightforward

estimation of charging time and state of charge (SOC) [34]. This can also be performed in two steps (CC-CC, figure 5b), where two different level constant currents are applied. Typically the first current (I_1 in the figure 5b) is higher to allow relatively faster charging [31]. When the voltage reaches a pre-set limit, the charging current is changed to a latter one (I_2 in the figure 5b) which is usually notably lower. This two-step approach helps to optimise the charging speed while also maximising the utilisation capacity of the system, which is important for analysing systems composed of solid boosters and charge-transporting solutions.

During constant voltage charging (figure 5c) voltage remains constant while the current is decreasing (starting typically from a notably high level of current) as the function of time. This process is more time consuming so it is usually used in systems where achieving a full charge requires a extended charging period [34]. However, this method requires very high starting currents which can be impractical with a real life application [31]. Furthermore, the high initial current and longer charging time can lead to battery degradation due to overcharging and unwanted heating of the battery [31, 34]. The final charging procedure is composed of CC and CP (figure 5d), it is a two-step method, where constant current is applied firstly and then constant voltage. Charging with CC until reaching pre-set voltage limit enables high charging rate, while charging with CP avoids overvoltage [34].

This analysis strategy provides qualitative information by visually analysing the charging/discharging profiles. For a quantitative examination, the following parameters can be obtained [31], which depend on the changes in current as a function of potential and time. The efficiency of a battery can be estimated when comparing the input energy upon charging with the output energy during discharging. Coulombic efficiency is the ratio of ampere-hours drawn from a battery when discharging and then when charging. In an ideal case, and after the discharge process, the battery should recover its original capacity. Voltage efficiency is the ratio of the average discharge voltage to average charge voltage. Energy efficiency refers to the portion of energy delivered when discharging from the energy used to charge the battery.

Coulombic efficiency (CE), voltage efficiency (VE) and energy efficiency (EE) can be determined by the following equations [35]:

$$CE = \frac{\int I_{dis}(t)dt}{\int I_{ch}(t)dt} \times 100\% \tag{6}$$

$$VE = \frac{\int V_{dis}(t)dt / \int V_{ch}(t)dt}{t_{dis}/t_{ch}} \times 100\% \tag{7}$$

$$EE = \frac{\int V_{dis}(t) I_{dis}(t) dt}{\int V_{ch}(t) I_{ch}(t) dt} \times 100\% \quad (8)$$

where V_{dis} and V_{ch} are the discharging and charging potentials, and I_{dis} and I_{ch} the discharging and charging current densities, respectively.

Upon charging, the total amount of current that the battery is able to store is referred as its storage capacity. Similarly, the capacity of the battery is the amount of charge that a fully charged battery can deliver. Both parameters are typically measured in ampere-hours (Ah). When comparing different batteries, it can be more informative to present their volumetric capacity, which is the capacity per unit volume, for example ampere-hours per litre (Ah L^{-1}).

Another important parameter is cycle life, which is the number of charge-discharge cycles that the battery goes through before its capacity drops (due to degradation, cross-over and/or Faradaic imbalance [36]) below selected performance criteria (often set at 80% of full capacity). Additionally, energy density refers to the energy output of the battery per unit mass or volume [31].

5 Proposal

Therefore, in this thesis, it was proposed to study flow batteries containing Prussian blue solid boosters in storage tanks, which are charged-discharged with a ferri-/ferrocyanide redox couple as charge-transporting intermediates. The performance of the systems will be evaluated with electrochemical techniques, such as cyclic voltammetry and a battery cycler through the application of CC, CP, CC-CC and CC-CP to charge-discharge flow battery cells of 5 cm^2 electrode area.

A cost-effective synthesis method for preparing solid particles without the use of expensive machinery will be developed. Different formulations for preparing solid boosters will be described and they consider varying ratios of carbon materials, KCl, and binder.

The best performing formulation will be used to study a FB with high concentration of charge-transporting species in a flow battery of 9 cm^2 of electrode area. The resulting system is expected to exhibit a utilisation capacity similar to or greater than that reported in the literature for PB solid boosters prepared with expensive equipment.

6 Procedures

The following section discusses the electrochemical techniques and chemicals used in this study.

6.1 Chemicals

All the chemicals used are commercially available. 1 mol L^{-1} KCl or 0.5/0.5 mol L^{-1} KCl/NaCl aqueous solutions were used as supporting electrolytes, and different ratios of the redox couple potassium ferrocyanide/ferricyanide ($K_4[Fe(CN)_6]^{4-/3-}$) were added to the solvent as electroactive materials to obtain charge-transporting solutions.

Solid boosters were prepared using PB and Poly(ethylene-co-acrylic acid) dissolved in tetrahydrofuran (THF) as active material and binder, respectively. KCl was added to the formulation to enhance porosity, and carbon black was utilised as a conductive material. Four different carbon materials were analysed, which are commercially available: YP-50F (Kuraray), YP-80F (Kuraray), BP2000 (Cabot) and CP65 (Nanografi).

6.2 Booster preparation

To prepare the boosters, the material ratios and procedure suggested by Balducci were considered [14]. All steps were performed under a fume hood. Wanted mass ratio of PB and CB were mixed together. As PEAA is in a form of clusters, it was first dissolved in THF and the resulted solution was added into the PB and CB mixture. In later experiments, KCl was also added to the PEAA and THF solution. The resulting mixture was left to dry for one hour maximum (time varied between 10 to 60 mins, depending on the carbon material) to form a

Figure 6: Solid boosters drying

paste. The paste was placed in an extruder (with several output holes of approximately 3mm) to make the boosters (figure 6). This method allows the cost-effective preparation of solid boosters without the need for expensive machinery. Resulting boosters were then left to dry under the fume hood overnight.

6.3 CV-test

Cyclic voltammogram tests were performed on the active materials potassium ferricyanide and PB, with a 0.1 Vs^{-1} scan rate. A Biologic ® (France) SP-240 multichannel potentiostat/galvanostat controlled by EC-Lab software, was used for the measurements. The counter electrode and reference electrode were a platinum wire and an aqueous Ag/AgCl (3 mol L^{-1} KCl) electrode, respectively. The ZIR tool was also linked to the process to automatically apply 95% IR drop compensation to the system. The obtained Ru values were approximately 10 ohms. A glassy carbon disk (diameter of 3 mm) was used as a working electrode. The working electrode´s surface was polished with 1 µm diamond powder from Büehler and then rinsed using distilled water, before each voltammogram was obtained. This procedure is exemplified in figure 3.

6.4 Battery test

FB cells assemblies contained in the middle two carbon current collectors and two carbon felt electrodes with geometrical area of 5 cm^2 and 9 cm^2. A piece of Nafion 212 cation-exchange

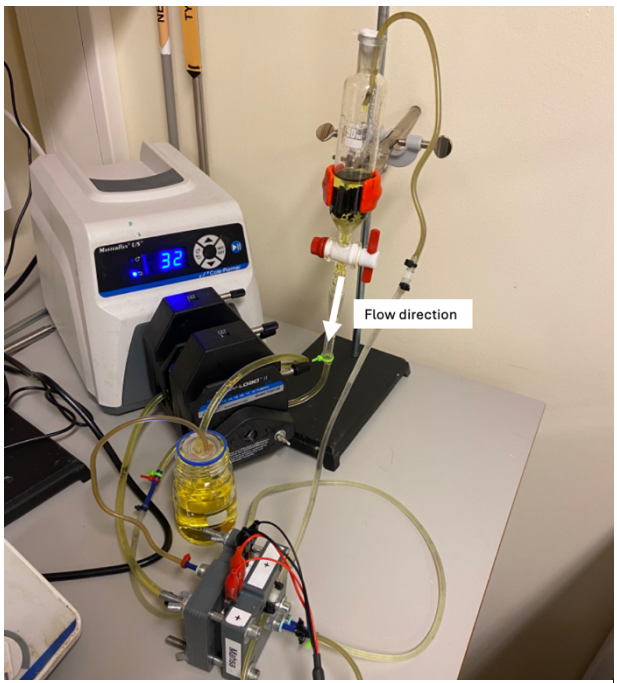

Figure 7: Schematic representation of the FB cell operating with solid boosters

membrane was placed in the middle on the cell to separate the latter two resulting electrodes, though which posolyte and negolyte solutions were pumped in recirculation mode with a Cole-Palmer peristaltic pump and Masterflex L/S pipe.

PB solid boosters were added into the negolyte reservoir. To prevent boosters from entering the cell and blocking the flow, glass wool was placed at the connection point between the tank and the pipe. The boosters were placed on top of the resulting bed. The operating principle of the designed system is shown in figure 7.

The system was galvanostatically charged-discharged using a battery testing system LANHE, Model G340A. It has the voltage range of -5 to 5 Volts and current ranges of 150 μA, 5 mA, 150 mA, and 5 A [37].

6.5 Scanning electrochemical microscopy

The cell consisted of a microelectrode (with diameter of 25 μm) as a WE, platinum wire as a CE and an aqueous reference electrode Ag/AgCl as a RE. The substrate was a solid booster material immersed in 100 mM potassium ferricyanide. The CHI900 SECM potentiostat was used for the measurements. A visual representation of the operating principle of this technique can be seen Moghaddam's thesis [21].

7 Results and discussion

Prussian White (PW) was introduced as an electroactive material to prepare solid boosters for improving the volumetric capacity of ferrocyanide flow battery posolytes [3, 6-7, 38]. Since the former compound was discontinued, it is usually synthesized by chemical reduction of Prussian Blue (PB), which involves purification and characterization methods [39]. As an alternative strategy, in this thesis, PW-based boosters were in situ obtained by reduction of PB-based particles in a downflow fixed bed reactor using electrogenerated ferrocyanide species (from ferricyanide species) in aqueous KCl solutions, as charge-transporting intermediates.

7.1 Analysis of the reversibility by voltametric stimulations

Considering a simple and reversible reduction process where n number of electrons are introduced into molecules O to form reduced species R (equation 9), the half way potential (10) of the system is determined by Nerns't equation (4). For a reversible one electron transfer process, the reactions are simplified as follows:

$$R \leftrightharpoons O + e^- \tag{9}$$

The reaction is controlled by the kinetic and thermodynamic parameters k_s and $E_{1/2}$ respectively, where k_s refers to electron transfer standard rate constant. The half way potential is determined by the following equation [30]:

$$E_{\frac{1}{2}} = \frac{E_c + E_a}{2} \tag{10}$$

where E_c and E_a are the cathodic and anodic peak potential values of the system, respectively.

The Butler-Volmer equation is also describing the I/E changes in cyclic voltammetry but different electrode conditions apply (equation 12). This equation describes the rate law of the system and relates the kinetic component of the forward and backward reaction $k_s = k_{s,1}/k_{s,2}$ (equation 13) with the current flowing through the electrode (i) as a function of the set potential [30].

$$i = nFA(k_{s,1}[O]_s - k_{s,2}[R]_s) \tag{11}$$

$$i = i_0(\exp\left[\frac{\alpha_a zF}{RT}(E - E^0)\right] - exp\left[\frac{\alpha_c zF}{RT}(E - E^0)\right]) \tag{12}$$

$$\Lambda_0 = \frac{k_s(\frac{D_O}{D_R})^{\alpha/2}}{(\frac{D_O \nu nF}{RT})^{1/2}} = \frac{k_s}{(\frac{D_O \nu nF}{RT})^{1/2}} \tag{13}$$

where A is the electrode area (in cm^2) and $[O]_s$ and $[R]_s$ concentrations of O and R at the surface of the electrode s, E is the electrode potential (in Volts), E^0 is the equilibrium potential (in Volts), α_a and α_c are anodic and cathodic charge transfer coefficients (normally, for reversible case $\alpha = 0.5$), respectively, D_O and D_R are the diffusion coefficients of the species O and R, respectively (typically $D_O = D_R = D$), z is the number of electrons, F is the Faraday constant, R is the molar gas constant, T is the temperature (in Kelvins) and v is the scan rate. For reversible systems species O and R are the equilibrium of the electrode surface. This condition can be achieved when k_s is big (e.g. 1 cms^{-1}) and/or the scan rate v is slow. Both properties are related through equation 13 with the dimensionless parameter Λ_0. Therefore, high values of Λ_0 refer to diffusion-controlled system. The reverse is true for irreversible ones.

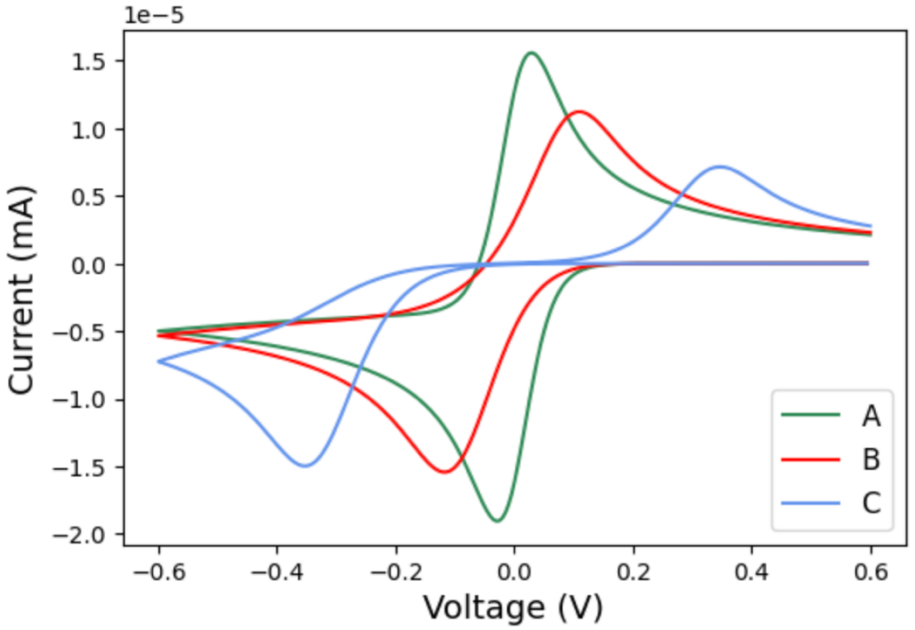

Figure 8: Simulated cyclic voltammograms for the reduction process of a single-electron transfer process of $D=1E^{-5}$ cm^2 s supposing $E_0 = 0$ V, concentration of 0.1 mol L^{-1} and electrode area of 7.1 mm^2. Variations are represented for $k_s = 1$ cm s^{-1} (A), 0.001 cm s^{-1} (B) and 0.00001 cm s^{-1} (C), for a scan rate of 0.1 V s^{-1}

To be able to analyse the cyclic voltammogram of the electroactive materials used in this study, a CV simulation was performed with software DigiElch 8F. The resulted voltammograms exhibited a typical behaviour detected in reversible, quasi-reversible and irreversible redox reactions. This information is useful for a visual analysis of reversibility in studied systems.

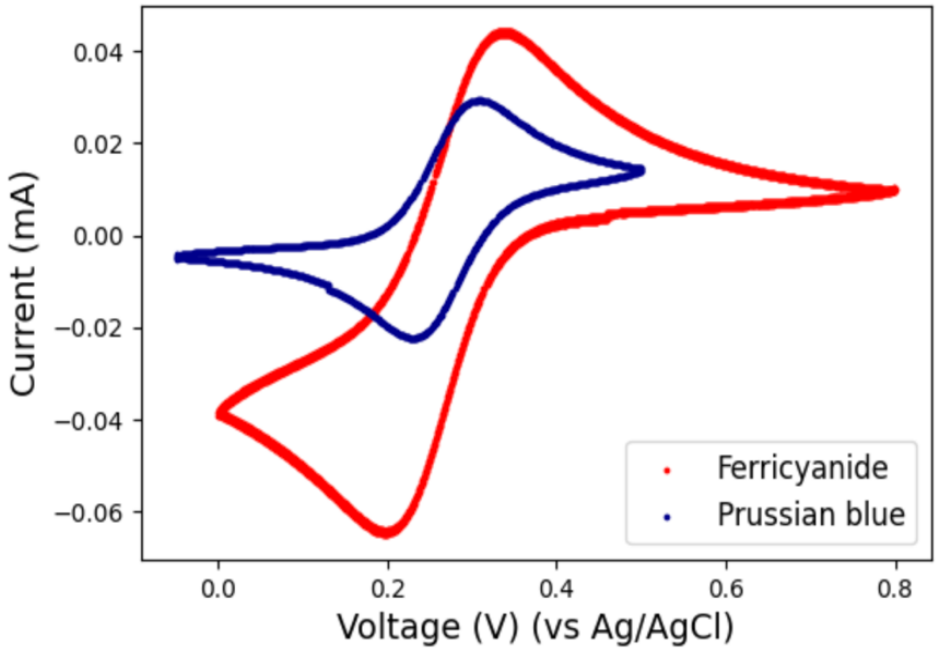

Figure 9: Cyclic voltammograms for the reduction process of 0.001 mol L^{-1} ferricyanide and Prussian blue in 1 mol L^{-1} KCl. Scan rate of 0.1 V s^{-1} and WE is glassy carbon (d=3mm)

Before preparing boosters, poorly (PB) and highly water-soluble (potassium ferricyanide) electroactive materials were examined by cyclic voltammetry. When comparing to the behaviour detected from simulations, it can be visually detected that the experimental voltammograms obtained from both solutions (Figure 9) exhibited reversible reduction processes at a relatively high redox potential, under the same thermodynamic condition. The electron transfer processes that occur in both compounds are described by equations 1 and 2. Therefore, the air-stable redox couples ferro/ferri and PB/PW were used as electroactive materials in the charge-transporting solution and booster particles, respectively. Boosters were prepared following a simple procedure introduced by Balducci [7]. The author studied different formulations and reported that boosters containing 70% and 65% electroactive material performed best. Similar systems were prepared and studied in the first part of this thesis. The first formulation (F1) analysed in a flow battery cell is the following: 70% PW, 20% carbon material BP2000, and 10% binder.

7.2 Carbon material effects on PB-based boosters' performance

Since the main objective of this thesis is the development of solid boosters to improve the volumetric capacity of posolyte solutions containing ferro/ferri redox couples, the systems were

therefore tested in a symmetric cell, which does not provide a battery with potential difference, but allows cycling stability studies. The long-term charge-discharge cycling stability of our F1-based boosters was tested in a FB cell by pairing the boosted tank in excess capacity to a ferrocyanide solution, as suggested by Balducci. The main motivation of this first stage was to examine the performance of the systems under conditions similar to those reported by the author.

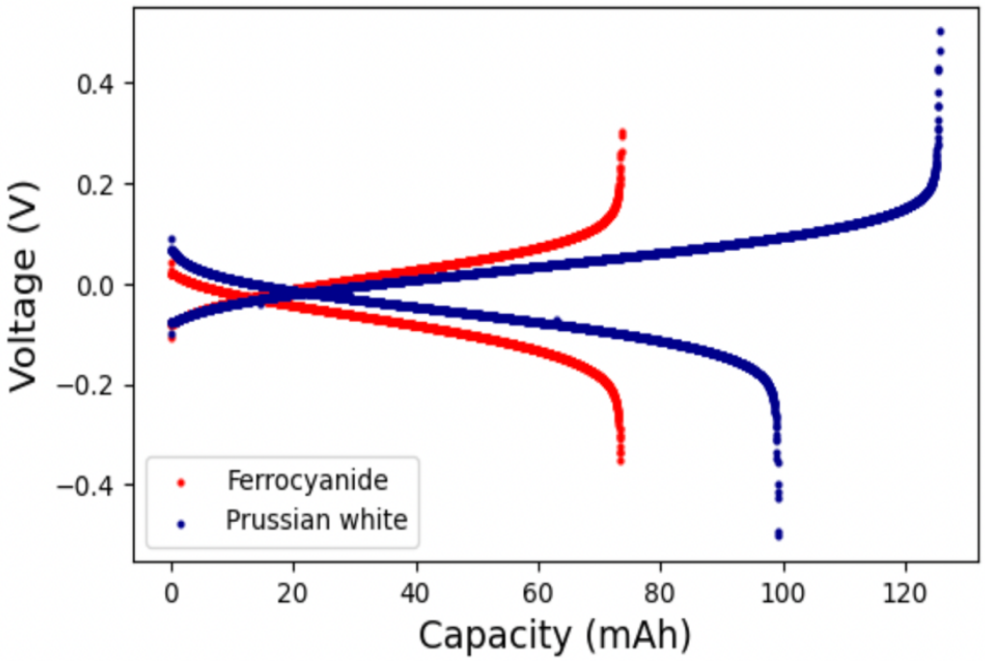

Figure 10: Charge-discharge capacity of the posolyte solution with (blue line) and without solid boosters (red line). Symmetric cell with 30 mL posolyte solution containing 0.003 moles of PW in boosters and 0.1 mol L^{-1} ferrocyanide in 1 mol L^{-1} KCl solution. The system was paired with 80 mL negolyte solution containing 0.1 mol L^{-1} ferrocyanide in 1 mol L^{-1} KCl

In the absence of solid boosters, the solution charged 75.9 mAh at a current density of 20 mA cm^{-2} (Figure 10), which is 92 % of the theoretical capacity (of the charge-transporting solution which was composed of 0.1 mol L^{-1} ferrocyanide) and is a similar percentage to that reported in the literature for ferrocyanide electrolytes of fast charge transfer kinetics [3, 6]. With the addition of solid boosters to the tank, the theoretical storage capacity was increased up to 402 mAh (321.6 mAh from boosters, considering that each PB molecule has a storage capacity of 4 electrons), the simplified electron transfer processes occurring at the boosters and electrolyte are described by equations 14 and 15, respectively.

$$PB + 4e^- \rightleftarrows PW \quad (14)$$

$$Fe(CN)_6^{3-} + e^- \rightleftharpoons Fe(CN)_6^{4-} \quad (15)$$

However, the improved system only charged 15.5 % of the booster´s capacity (125.6 mAh), which is a very low value compared to the literature [3, 6]. The capacity was limited by the other tank (214 mAh), as was also detected from Balducci's results. Additionally, the system discharged less than expected.

As a result, the system immediately lost a significant amount of its storage capacity in the first charge-discharge cell cycles, utilizing practically the storage capacity of the electrolyte as the test progressed.

The long-term cycling stability of posolyte solutions containing ferro/ferri redox couples has been widely demonstrated. So, the problem detected here must be related to the boosters. Since no significant deterioration of the particles was visually detected, there was a possibility that the electroactive material PB evolved towards an irreversible reduction process upon charging the cell. Although this is very different from what has been reported in the literature.

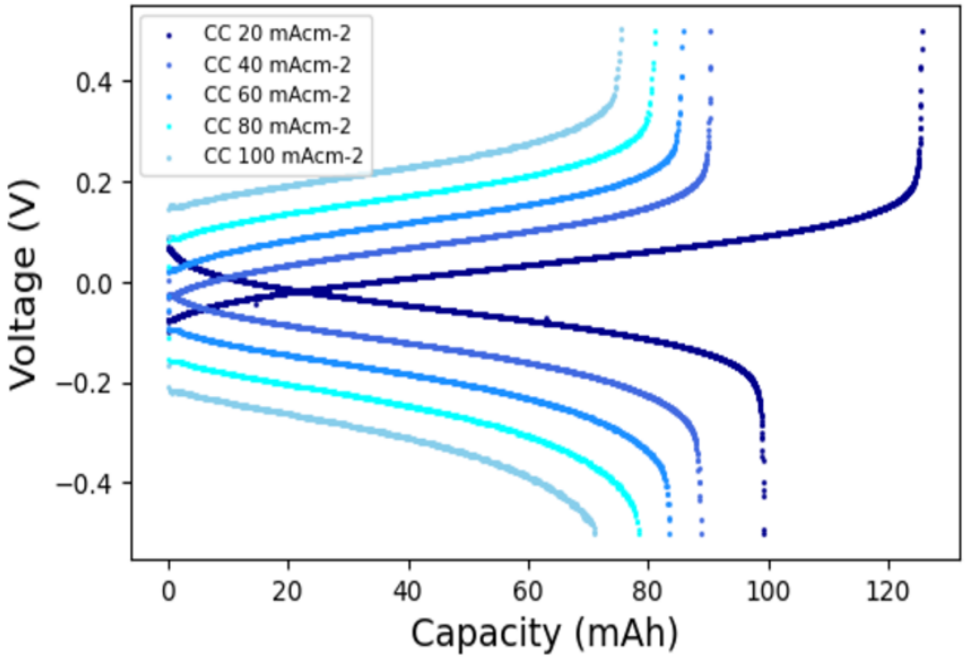

Figure 11: Charge-discharge capacity at different constant current densities (CC) for a symmetric cell assembled with 30 mL posolyte tank containing 0.003 moles of PW in the boosters and 0.1 mol L^{-1} ferrocyanide in 1 mol L^{-1} KCl solution. The system was paired to 80 mL negolyte solution containing 0.1 mol L^{-1} ferrocyanide in 1 mol L^{-1} KCl

When changing the current density in the system (Figure 11), it was detected that, capacity loss is greater as the cell is charged-discharged faster, then an irreversible degradation mechanism of material cannot be invoked. In other words, the system´s capacity should start to recover as the charge-discharge speed increases, since under these conditions the material probably does not have enough time to evolve towards irreversible pathways. Since no evidence of material degradation was found, as another alternative, it was proposed to evidence a slow kinetics at the electrolyte-booster interface, which makes sense since the batteries reported at the moment were cycled with long charge-discharge times [3, 6]. For this purpose, a combined program was used incorporating the application of constant current (60 mA cm^{-2} with limit to ±0.6 V) followed by constant voltage (0.6 V potential with limit to 6 mA). Note that this strategy requires more time for charging-discharging the cell, but allows working with the maximum utilisation capacity of electroactive materials.

Table 1: Properties of four different carbon black materials

Carbon material	**Density (g cm^{-3}) at 20 °C**	**Surface area (m^2 g^{-1})**
BP2000	1.7-1.9	1500
YP-50F	0.30	1692
YP-80F	0.18	2271
C65	0.16	62

The intercalation reaction (with positive ions) that is coupled to the electron transfer process when charging the boosters is likely constrained by a relatively low porosity (probably the binder is negatively affecting this property) of the material, which leads to a slow charge transfer kinetics. To improve porosity, we proposed incorporating KCl into the formulation when preparing the boosters. KCl species should dissolve in contact with water and no longer be part of the boosters, creating holes that favour mass transport through the particle. With these changes the formulation resulted as follows: 65% PB, 10% carbon, 15% KCl and 10% binder.

As the effect of carbon type on booster´s performance has not been reported, in this work, 4 different carbon materials were considered for the formulation, whose main properties were compiled in Table 1. The 4 resulting booster formulations were charged-discharged (with a CC-

CP procedure using 0.1 mol L^{-1} ferricyanide) with a symmetric cell in tanks containing a theoretical booster capacity of 321.6 mAh. The results obtained are summarized in Figure 12.

With these considerations, it was possible to charge-discharge boosters with 4 different materials for a significant number of operating cycles, which reinforces the fact that the charging-discharging process of these systems is not evolving towards an irreversible side reaction, but is limited by a slow electron transfer kinetics at the electrolyte-booster interface. The sudden increase in capacity with YP-80F and BP2000 carbon materials is due to the fact that the contact between the boosters and solution at the storage tank was adjusted. This happened when it was noticed that in some cases a significant number of particles were floating and not coming into contact with the liquid.

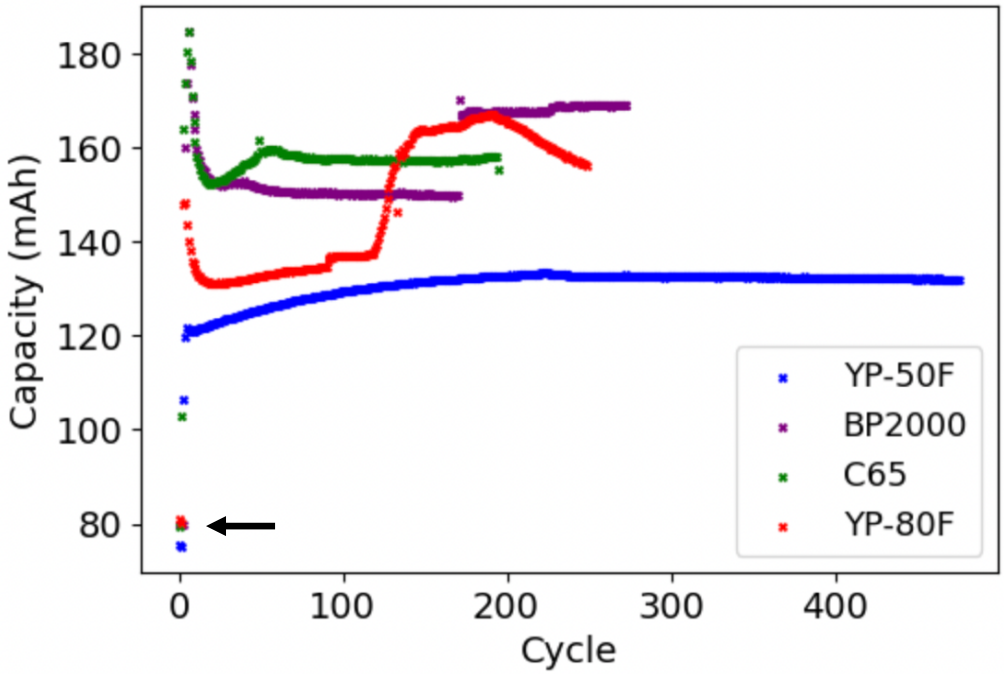

Figure 12: Discharge capacity for boosters prepared with 4 different carbon materials. Symmetric cell assembled with 30 mL negolyte solution containing boosters with 0.003 moles of PB in boosters and 0.1 mol L^{-1} ferricyanide in 1 mol L^{-1} KCl. The system was paired to 80 mL negolyte solution containing 0.1 mol L^{-1} ferrocyanide and 0.01 mol L^{-1} ferricyanide in 1 mol L^{-1} KCl. Charging process was CC 60 mA cm^{-2} with limit to ±0.6 V and CP (0.6 with limit to 6 mA). The arrow is pointing to capacity before adding the boosters (solution capacity).

For material YP-80F, a dramatic decrease in storage capacity was also detected after cycle 194, and this is due to the fact that we added 1 mL of methanol to the system. The idea was to try to modulate the redox potential of electroactive species with alcohol-water mixtures. However, the additive generated negative effects; so, this strategy was immediately discarded for other systems.

It's worth mentioning that the cycling stability of solid boosters has been demonstrated with FBs operating for more than 1000 charge-discharge cycles [3]. In fact, some of our systems also achieved similar stability, and a very important result of our work is that, a simple booster manufacturing strategy is being introduced that do not involve the use of expensive equipment, something that had not been considered until now. The idea was initiated by our group with Balducci [7], but the long-term cycling stability of the resulted boosters remained to be demonstrated, as the author was only able to test batteries for maximum 41 charge-discharge cell cycles.

From Figure 12, a significant effect of the type of carbon material on the storage capacity of the boosters was detected as well, but no property (Table 1) was found that describes the observed trends: with BP2000, YP-80F, YP-50F and C65 carbon materials, the utilisation capacity of the boosters turned out to be 34.0 %, 26.6 %, 17.3 % and 32.9 %, respectively.

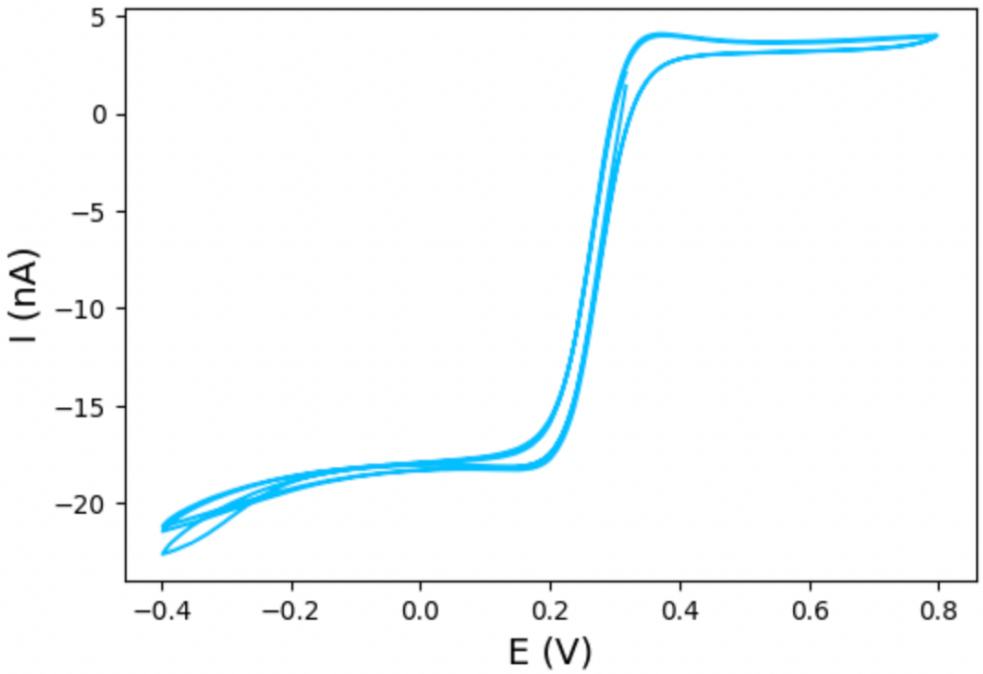

Figure 13: Cyclic voltammogram for the reduction process of 0.1 mol L^{-1} ferricyanide in 1 mol L^{-1} KCl with an ultramicroelectrode (d=25 μm^2). Scan rate: 50 mV s^{-1}. E vs Ag/AgCl

In the attempt to investigate the effect of carbon materials on the performance of PB solid boosters, scanning electrochemical microscopy (SECM) experiments were performed, as proposed by Moghaddam [21]. The applied potential, 0 V, was measured in a similar manner than in conventional electrochemical cells using cyclic voltammetry (figure 13). However, in this case, the working electrode is a platinum microelectrode with a diameter of 25 µm.

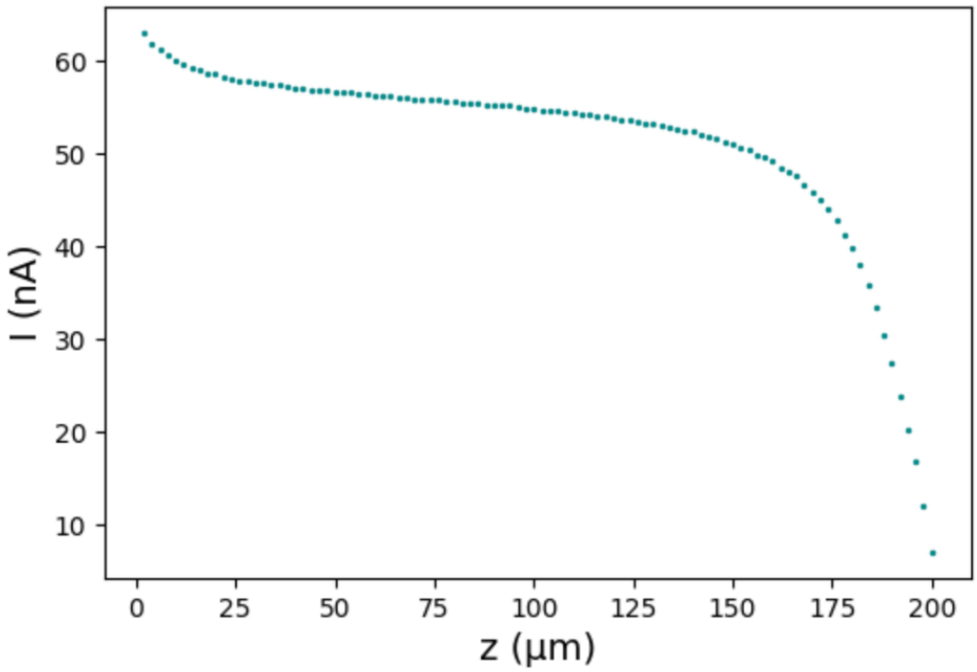

Figure 14: SECM approaching curve for a copper tape in 0.1 mol L^{-1} ferricyanide and 1 mol L^{-1} KCl. Approaching speed was 50 µm/s. The potential applied at the electrode surface was 0.6 V. At the beginning the distance of the electrode from the surface was 200 µm.

To determine the expected behaviour, the approaching curve was first tested with a copper tape. As illustrated in figure 14, the results show that as the electrode approaches to the copper surface, the current is heading towards more negative values.

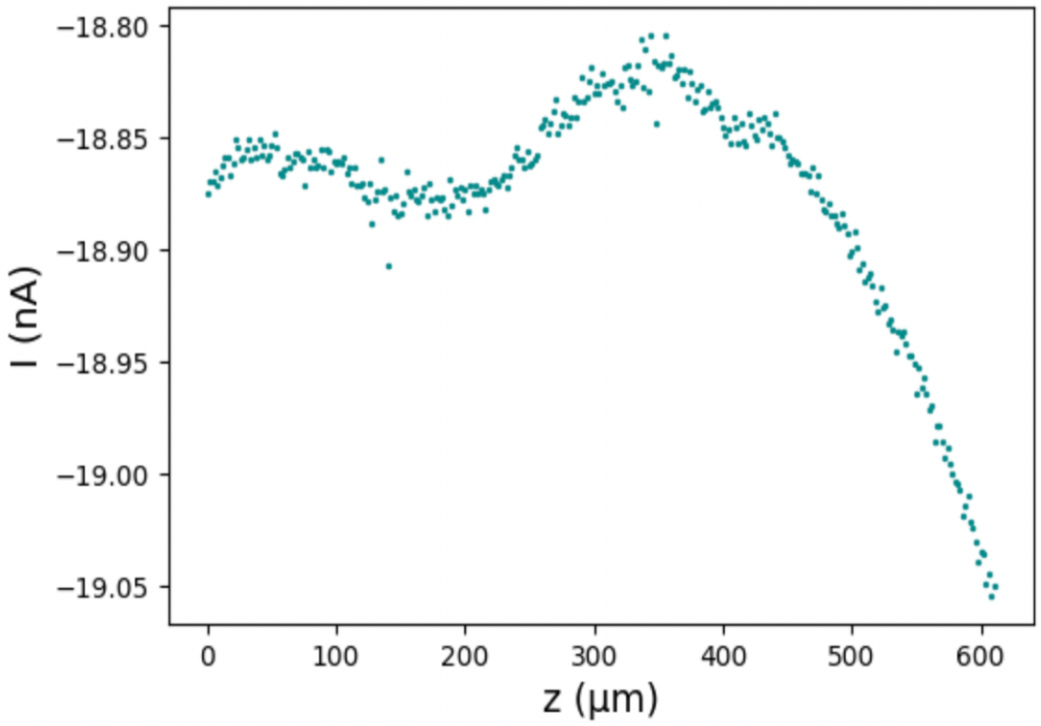

Figure 15: SECM approaching curve for solid booster ink with yp-50F carbon material in 0.1 mol L^{-1} ferricyanide and 1 mol L^{-1} KCl. Approaching speed was 50 µm/s. The potential applied at the electrode surface was 0 V. At the beginning the distance of the electrode from the surface was 600 µm.

A similar trend was expected when approaching the microelectrode to an ink prepared with a similar formulation than the boosters. Although, it was possible to detect the electrocatalytic activity of the boosters in one of the tests (evidenced by an increase in current toward negative values when approaching the electrode, in figure 15), the results were not reproducible. In addition, for the remaining systems an opposite trend was detected when approaching the ink material with the microelectrode, which is inconsistent according to the redox reaction under investigation here (equations 14 and 15). When preparing inks, it was observed that achieving uniform flat surfaces is particularly difficult. So, it is proposed that reproducible results could be obtained with this technique if a method is developed to prepare the booster material in a way that creates uniformly flat ink layer, which better suits to the micro size approach. In some cases, the approaching experiment on non-flat surfaces resulted in the microelectrode breaking. So, it is notable that further analysis with SECM could provide relevant information on the electrochemical kinetics at the booster material surface and as a result, a better understanding of the carbon material effects on the boosters performance could be achieved.

In general, a low utilisation capacity was observed for all cases studied because, with the experimental conditions proposed by Balducci [7], the overall system capacity is limited by the tank (214.4 mAh) not containing boosters. Surprisingly, the carbon material (YP-50F) offering lowest utilisation capacity (17.3 %) was the most stable upon cycling. The rest of the systems were dissolved before reaching 400 cycles, blocking the flow. Therefore, it is promising to continue working on improving the performance of the YP-50F-based system.

7.3 Solid booster discharge time depending upon carbon material

To examine the booster´s performance as a function of charging-discharging time, the systems were also tested under conditions where the tank not containing boosters had excess storage capacity. A similar formulation was considered for preparing the boosters, but only BP2000 and YP-50F carbon materials were investigated in the first step. The boosted tank had 294 mAh of theoretical storage capacity, of which 160 mAh came from boosters and the rest from the charge-transporting solution.

In the first 100 charge-discharge cycles (Figure 14), both systems exhibited a similar behaviour working with approximately 10% (YP-50F) and 13% (BP200) of the boosters' utilisation capacity for energy storage. However, after cycle 100, the capacity of the systems began to differ, but always raising without reaching a limit value for a maximum charge-discharge storage capacity. In fact, the maximum capacity achieved was 203 mAh (74,8 mAh from the

boosters) for the system developed with BP2000 carbon material, which represents 46.8 % of the theoretical storage capacity of the PB-based boosters (4-electron storage capacity per PB molecule).

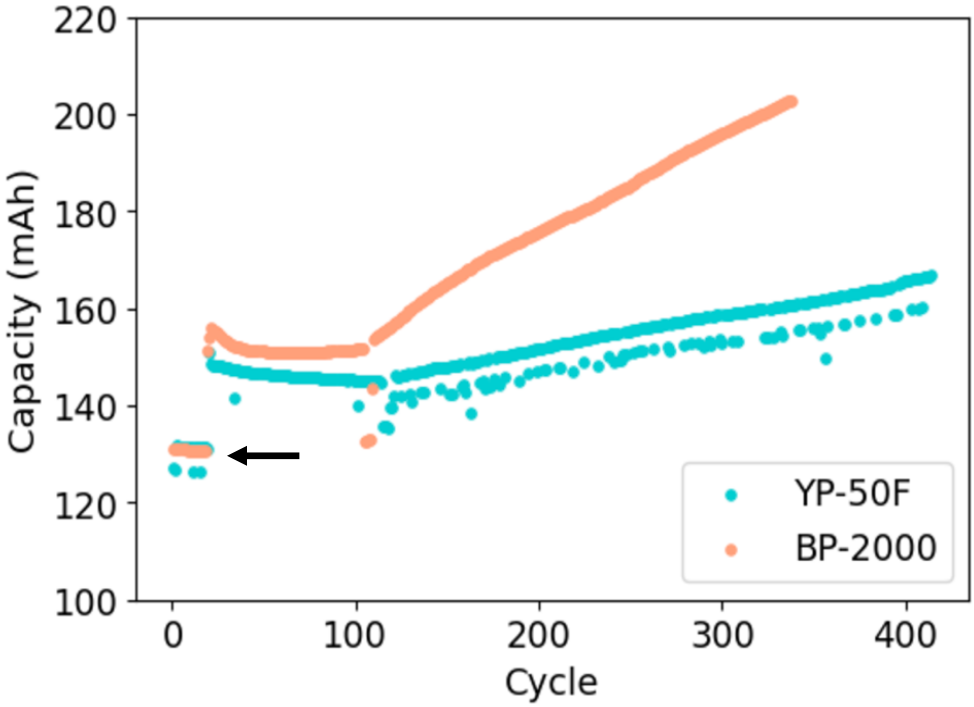

Figure 14: Representation of the charge-discharge capacities for boosters prepared with different carbon materials. Symmetric cell assembled with 25 mL negolyte solution containing 0.005 moles of PB in boosters and 0.2 mol L^{-1} ferricyanide in 1 mol L^{-1} KCl solution. The system was paired to 65 mL posolyte solution of 0.2 mol ferrocyanide and 0.02 mol L^{-1} ferricyanide in 1 mol L^{-1} KCl. Charging-discharging with CC ±60 mA cm^{-2}, cut off ±0.5 V, and then with CP (0.6 with limit to 6 mA). The arrow is pointing the experimental capacity of the solution, before adding the boosters.

This utilisation capacity remains significantly lower than that reported in the literature for similar systems, e.g. 61.0 % as reported by Yan et al. [3] and 73.5 % reported by Chen et al.[6], but it has improved. For the case of carbon material BP2000, the increased capacity detected upon cycling the cell seemed to show a promising system, but this phenomenon was accompanied by a physical deterioration of the solid particles, which released powder into the pipes and blocked the flow, causing leakage and battery failure. In contrast, the slight increase in capacity detected for system containing YP-50F did not result in cell cycling failure, which is also an indicator that it is promising to continue working on improving this last formulation. Therefore, the test was not repeated for the other two carbon materials. Instead, it was decided to increase the amount of binder content from 10% to 15%, while decreasing the amount of KCl from 15% to 10%. This adjustment aimed to see whether a higher binder amount could prevent a severe degradation of the boosters, although it could potentially have negative effects on the

charge transfer kinetics at the booster interface. Four variants of carbon materials were again needed to obtain different particle characteristics.

Battery tests were conducted for each carbon-based booster preparation. They were submitted to three different charging-discharging programs consecutively, using the same assembled system (for each carbon material) for all the tests. The goal was to identify methods for optimising the testing time, without significantly compromising the utilisation capacity and efficiency of the system.

The first program involved consecutively applying CC(fast)-CC(slow) charge-discharge current densities of ±70 mA cm^{-2} and ±3 mA cm^{-2} for over 40 cycles. For preparing the boosted tanks, a theoretical capacity of 375.2 mAh was considered, where half of the capacity came from boosters. In these cases, the concentration (0.35 mol L^{-1}) of ferricyanide in the charge-transporting solution was higher than in the previous tests, and excess capacity was also placed in the tanks paired to the boosted tanks for testing.

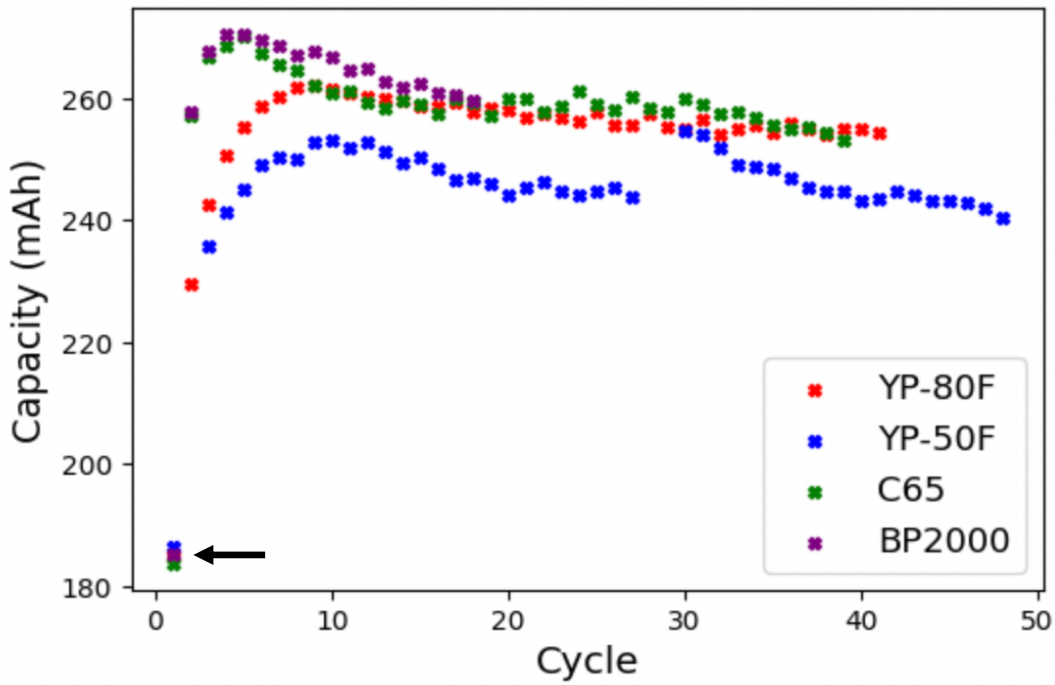

Figure 15: Representation of charge-discharge capacity of the boosters prepared with different carbon materials. Symmetric cell assembled with 20 mL negolyte solution containing 0.007 moles of PB in boosters and 0.35 mol L^{-1} ferricyanide in 0.5 mol L^{-1} KCl and 0.5 mol L^{-1} NaCl solution. The system was paired to 55 mL posolyte solution of 0.35 mol L^{-1} ferrocyanide and 0.035 mol L^{-1} ferricyanide in 0.5 mol L^{-1} KCl and 0.5 mol L^{-1} NaCl solution. Charging-discharging with CC ±70 mA cm^{-2} with limit to ±0.5 V and CC 3 mA cm^{-2} (with limit to ±0.55 V). The arrow is pointing the capacity of the solution, before adding the boosters.

To prepare charge-transporting solutions, ferri/ferro electroactive materials were dissolved in 0.5 mol L^{-1} NaCl + 0.5 mol L^{-1} KCl. The mixture of counterions improves the water solubility

of ferri/ferro redox couples [19], and probably favour the intercalation process (since Na^+ intercalating species are smaller than K^+ species) at the booster particles upon cycling the cell. The achieved capacities and cycle duration corresponding to each carbon material are shown in figure 15 and table 2, respectively.

Table 2: Cycle duration for each carbon material

Carbon material	Cycle duration (h)
BP2000	11,1
YP-50F	6,7
YP-80F	8,3
C65	7,1

The storage and utilisation capacities achieved for boosters prepared with the carbon materials BP2000, YP-80F, YP-50F and C65 were 86.3, 78.1, 69.3 and 86.2 mAh, corresponding to 46.0 %, 41.6 %, 36.9 % and 45.9 %, respectively. Differences in cycle count are only due to switching to the next program on a different cycle. Once again, the battery containing boosters prepared with the carbon material BP2000, suffered severe degradation causing its booster material to travel into the cell, which led to battery leakage and failure. This test was repeated three times and the boosters always dissolved. The best result obtained for the latter case is shown in figure 15.

As seen from table 2, the cell with boosters containing carbon material YP-50F had fastest cycle duration of 6,7 hours. However, (figure 15), the plot exhibits a lowest utilisation capacity of the boosters in this case. By incorporating the carbon material C65 in the system, the utilisation capacity can be significantly improved without greatly affecting the discharging time of the boosters (from 6.7 to 7.1 hours). The problem with this system is its poor cycling stability. The remaining carbon materials provided a relatively high utilisation capacity, but the charge-discharge times increased considerably. As expected, all the systems exhibited a columbic efficiency close to 100%, as shown in figure 16.

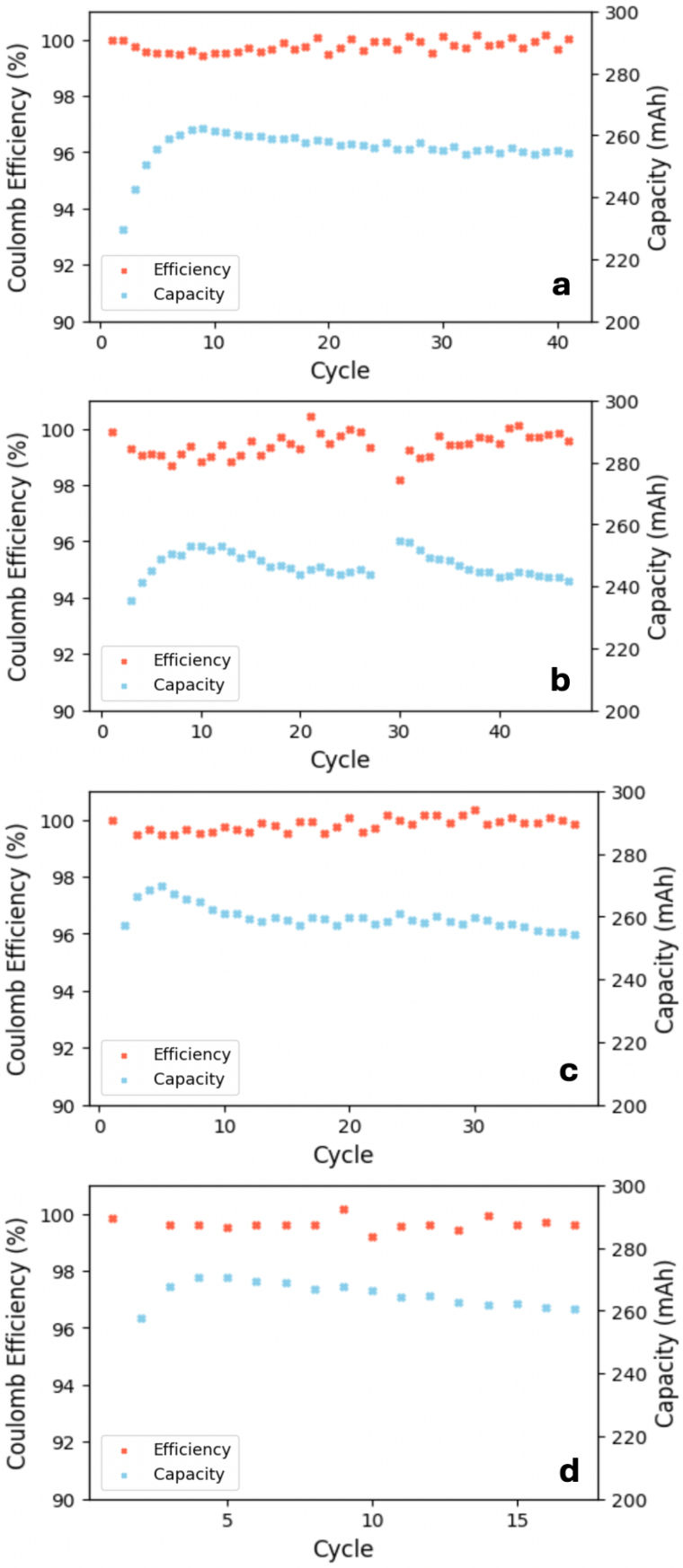

Figure 16: Galvanostatic cycling parameters for a symmetric cell assembled with 20 mL negolyte solution containing 0.007 moles of PB in boosters and ferricyanide and 0.35 mol L^{-1} ferricyanide in 0.5 mol L-1 KCl and 0.5 mol L^{-1} NaCl solution. The system was paired to 55 mL posolyte solution of 0.35 mol L^{-1} ferrocyanide and 0.035 mol L^{-1} ferricyanide in 0.5 mol L^{-1} KCl and 0.5 mol L^{-1} NaCl solution. Charging process was CC 70 mA cm^{-2} with limit to ±0.5 V and CC 3 mA cm^{-2} (a) YP-80F, (b) YP-50F, (c) C65, (d) BP200.

As a second strategy, the same cycled cells were examined as a function of different current densities, during 10 charge-discharge cell cycles for each current density. The selected values were ±72, ±60, ±48, ±36, ±24, ±12, ±6, ±3 mA cm^{-2} for a single-step CC process programmed for charging-discharging the cell.

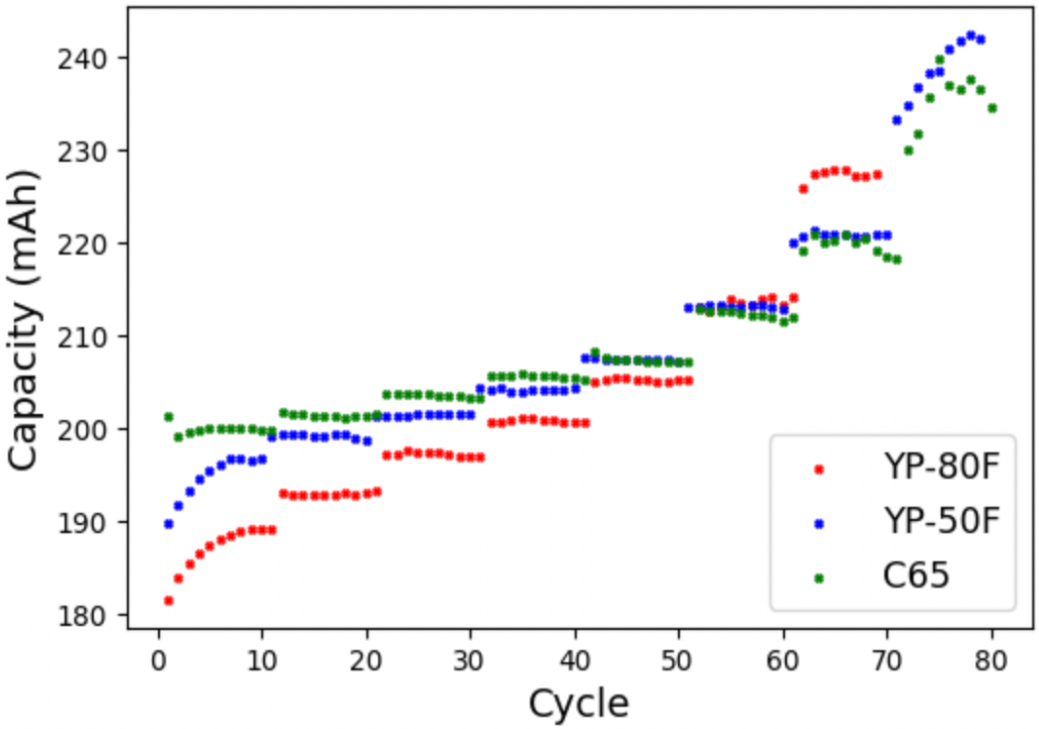

Figure 17: Representation of the charge-discharge capacity of boosters prepared with different carbon materials. Symmetric cell assembled with 20 mL negolyte solution containing 0.007 moles of PB in boosters and ferricyanide in 0.5 mol L^{-1} KCl and 0.5 mol L^{-1} NaCl solution. The system was paired to 55 mL posolyte solution of 0.35 mol L^{-1} ferrocyanide and 0.035 mol L^{-1} ferricyanide in 0.5 mol L^{-1} KCl and 0.5 mol L^{-1} NaCl solution. Charging-discharging with CC with decreasing current density varying between ±72 mA cm^{-2} and ±2 mA cm^{-2} with limit to ±0.55 V (ten cycles each).

The intention behind the second program was to see how much increasing the charging speed affects the utilisation capacity of the boosters. The results obtained with three different carbon materials are presented in figure 17, as the boosters prepared with carbon material BP2000 degraded during the first state of testing.

As expected, with increasing the current density in all the systems studied resulted in lower utilisation capacity values for the boosters. Actually, at the highest current density tested, only the storage capacity of the charge-transporting solution is utilised. For the carbon materials YP-80F, YP-50F and C65, the energy storage capacities (data estimated at current densities ±6mAh and ±3mAh) in the boosters were 42.9, 55.9, and 51.9 mAh, corresponding to 22.9 %, 29.8 %, and 27.7 % of the boosters' theoretical utilisation capacity, respectively. These results further support the fact that the kinetics at the interface between the solid particle and the charge-transporting solution is the rate determining step.

In this case (figure 17), all the systems exhibited a similar storage capacity. One thing that stands out is that the boosters prepared with carbon material YP-50F exhibited the lowest utilisation capacity in the previous test (figure 15), where charging-discharging quickly was not an important factor, but with second program, it is now very similar in comparison with the remaining systems examined. Therefore, the experimental results obtained in this thesis reveals that, although the carbon material YP-50F decreases the utilisation capacity of the PB solid boosters in FBs, it also provides a long-term cycling stability of the particles without significantly affecting the electron transfer kinetics at the booster's surface. For the remaining cases, the kinetic component is relatively low and indeed, the utilisation capacity of the PB material in those particles is significantly decreasing when increasing the charge-discharge speed. These results also highlight that the most effective system developed in this thesis is the one containing the YP-50F carbon material.

It should be highlighted, that this system suffered from leaking because the pipe was broken (at the non-booster side), causing a charge imbalance in the cell. Despite this, the system could be restored by adding a new solution and replacing the piping in the affected tank. The system

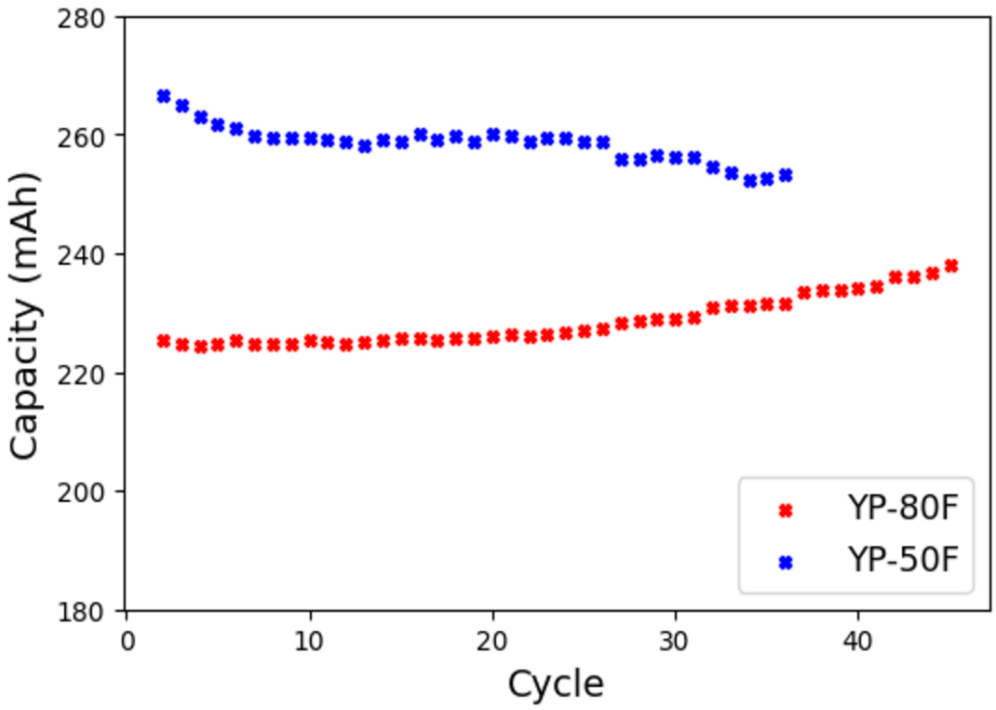

Figure 18: Representation of the charge-discharge capacity of boosters prepared with different carbon materials. Symmetric cell assembled with 20 mL negolyte solution containing 0.007 moles of PB in boosters and ferricyanide in 0.5 mol L^{-1} KCl and 0.5 mol L^{-1} NaCl solution. The system was paired to 55 mL posolyte solution of 0.35 mol L^{-1} ferrocyanide and 0.035 mol L^{-1} ferricyanide in 0.5 mol L^{-1} KCl and 0.5 mol L^{-1} NaCl solution. Charging-discharging with CC-CC, first CC with decreasing current density varying between ±72 mA cm^{-2} and ±2 mA cm^{-2}, cut off ±0.55 V (ten cycles each), following each time with CC ±2 mA cm^{-2}, cut off ±0.55 V

prepared with carbon material C65 also presented a leakage, but in this case the boosters degraded and the material travelled into the cell.

Finally, the third procedure was applied, which is similar to the second test. 10 charge-discharge cell cycles were examined though a CC-CC program for every different current density applied with cut off values of ± 0.55 V: ±72, ±60, ±48, ±36, ±24, ±12, ±6, ±3 mA cm^{-2}. For every value, both charging and discharging processes were followed by an immediate application of 2 mA cm^{-2}.

This program was performed for those systems containing carbon materials YP-80F and YP-50F, which did not degrade in the previous tests, unlike the remaining systems. Under these conditions, (Figure 18), the boosters containing carbon material YP-80F performed as expected, achieving an energy storage capacity of 52.3 mAh (which corresponds to a capacity utilisation of 27.9 %). Surprisingly, the boosters prepared with carbon material YP-50F apparently exhibit the opposite behaviour, storing more energy (80.1 mAh) and reaching an utilisation capacity of 42.7%. This result is in line with those from the previous tests, suggesting that the carbon material YP-80F negatively affects the electron transfer kinetics on the surface of the boosters. In the case of the system assembled with carbon material YP-50F, its kinetics remains significantly fast which allows it to charge faster. As a result, it does not experience significant effects when changing the rate of charging-discharging, and it benefits from having high concentrations of ferrocyanide in the solution, since the charging mechanism of the boosters requires 4 molecules of charge-transporting species to charge every molecule of PB. In systems with slow electrode kinetics, this increase in concentration of ferri/ferro redox couple does not allow the charge-discharge process to be accelerated.

The above results clearly demonstrate that the effective concentration of electrogenerated species in solution is key for successfully charging-discharging the boosters at the storage tanks. However, the results also suggest that this advantage cannot be achieved if the systems experience a relatively slow kinetics on the surface of the boosters.

To rationalise this effect, the charge storage capacity of the latter two discussed systems was examined with two different processes; applying ±70 mA cm^{-2} followed by ±3 mA cm^{-2}; and applying just ±3 mA cm^{-2}. Both systems exhibited (Figure 19) similar energy storage capacities when charging quickly, as this condition leads to fast accumulation of electrogenerated species in solution. However, charging slowly (applying 3 mA cm^{-2}) negatively affected the energy storage capacity of the cell containing boosters fabricated with carbon material YP-80F,

resulting in a lower capacity with this approach. This phenomenon happens because there is no immediate effective concentration of reduced species and the kinetics at the booster region appear to be slow, and four reduced species are required to charge every molecule of PB. The reverse is true for the system containing carbon material YP-50F, where the storage capacity remains similar for both charging-discharging strategies.

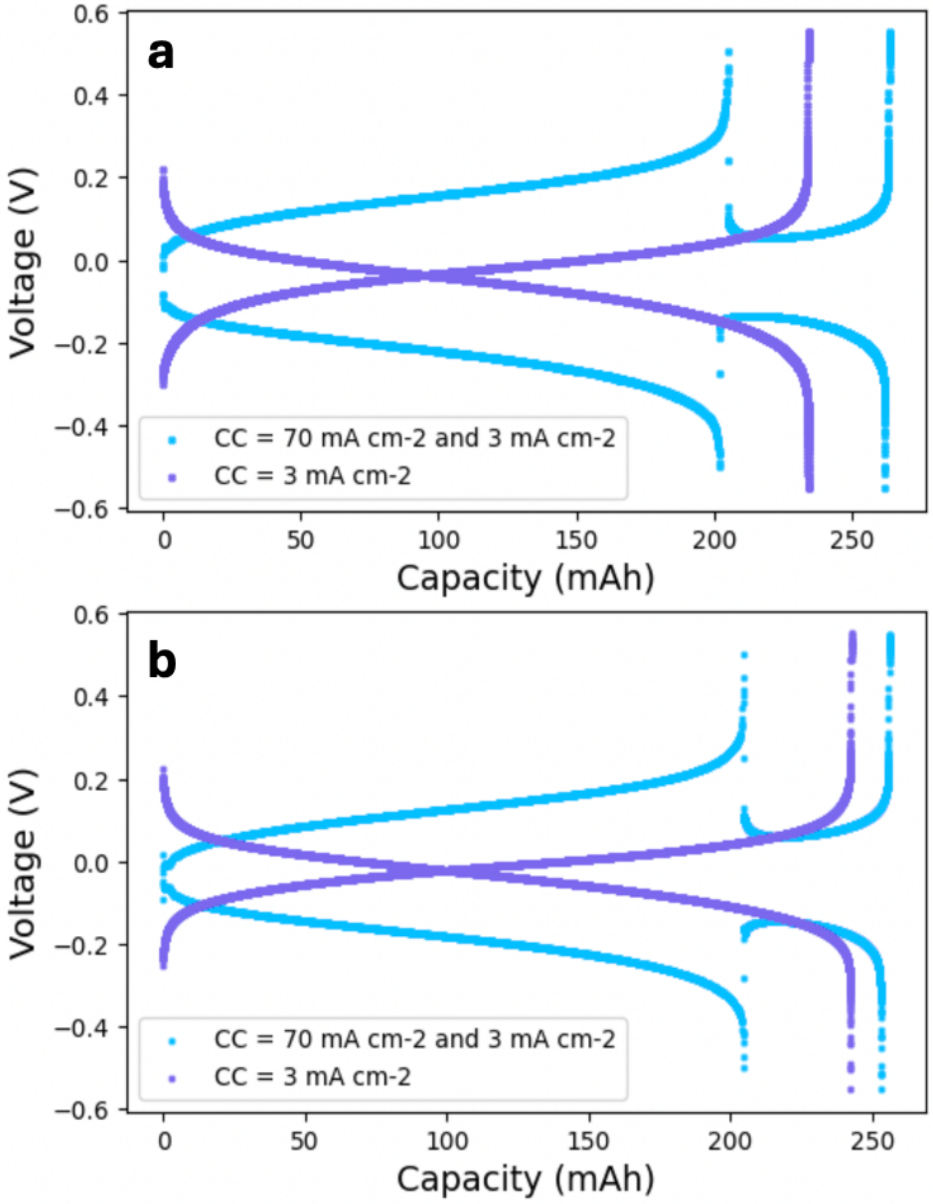

Figure 19: (a) Representation of capacity change with different charging speeds. Symmetric cell assembled with 20 mL negolyte solution containing 0.007 moles of PB in boosters and ferricyanide and 0.035 mol L^{-1} ferrocyanide in 0.5 mol L^{-1} KCl and 0.5 mol L^{-1} NaCl solution. The system was paired to 55 mL posolyte solution of 0.35 mol L^{-1} ferrocyanide in 0.5 mol L^{-1} KCl and 0.5 mol L^{-1} NaCl solution. Boosters contain carbon material YP-80F. (b) Same than a, but with carbon material YP-50F

To demonstrate the effect of the concentration of ferri-ferro redox couples on the charging process of YP-50F system, battery cell experiments with a larger electrode area are required. Otherwise the experiment would take a long time.

7.4 Improved utilisation in YP-50F system

In summary, it's evident that adding PB solid boosters improve the energy storage capacity in FB electrolytes containing ferri-/ferrocyanide redox active species, as also demonstrated above [3], [6]. Furthermore, as seen in figures 12 and 17, increasing the concentration of the charge transporting species also enhances the utilisation capacity of the boosters. For example, with carbon material BP2000 the highest utilisation capacity of boosters was 34.0% (figure 12) at a 0.1 mol L^{-1} concentration of ferricyanide. The utilisation capacity increased to 46.0% (figure 17) when the concentration was raised to 0.35 mol L^{-1}.

Despite this increase, the utilisation capacity still remains significantly lower than the values reported in the literature: Yan et al. and Chen et al. reported 61.0 % [3] and 73.5 % [6], respectively. Nevertheless, a direct comparison of the results in this study to those previously published is not straightforward. These studies mentioned tested bigger batteries, which enable the addition of higher concentrations of the charge-transporting species and at least in this thesis it was shown that the concentration of this component also significantly impacts the charge capacity of the PB solid boosters. However, employing similar concentrations of the charge-transporting species is not practical with cells of small electrode area, such as those presented in the previous sections of this thesis, because it would take a long time during each charge-discharge cycle. Additionally, small electrode areas often result in a significant increase in the system's overpotential when the material is rapidly charged-discharged with high current densities. This occurs because an effective equilibrium cannot be established between the electrogenerated species moving away from the electrode and the molecules traveling toward the electrode surface to undergo transformation [29, 32].

To assess the utilisation capacity of the systems studied in this thesis, under charge-transporting species concentrations similar to those reported, a FB cell with larger-area (9 cm^2) electrodes was used to continue the investigations. With this configuration, the effective concentration of electrogenerated species in the charge-transporting solution is expected to increase further, without the need for unpractically long charge-discharge times.

In this final stage, boosters with the best characteristics in terms of utilisation capacity and cycling stability were tested, and they have the following composition: 65% PB, 10% carbon material YP-50F, 15% KCl and 10% binder. The concentration of the charge transporting species was increased to 0.8 mol L^{-1} and the results obtained are presented in figure 20.

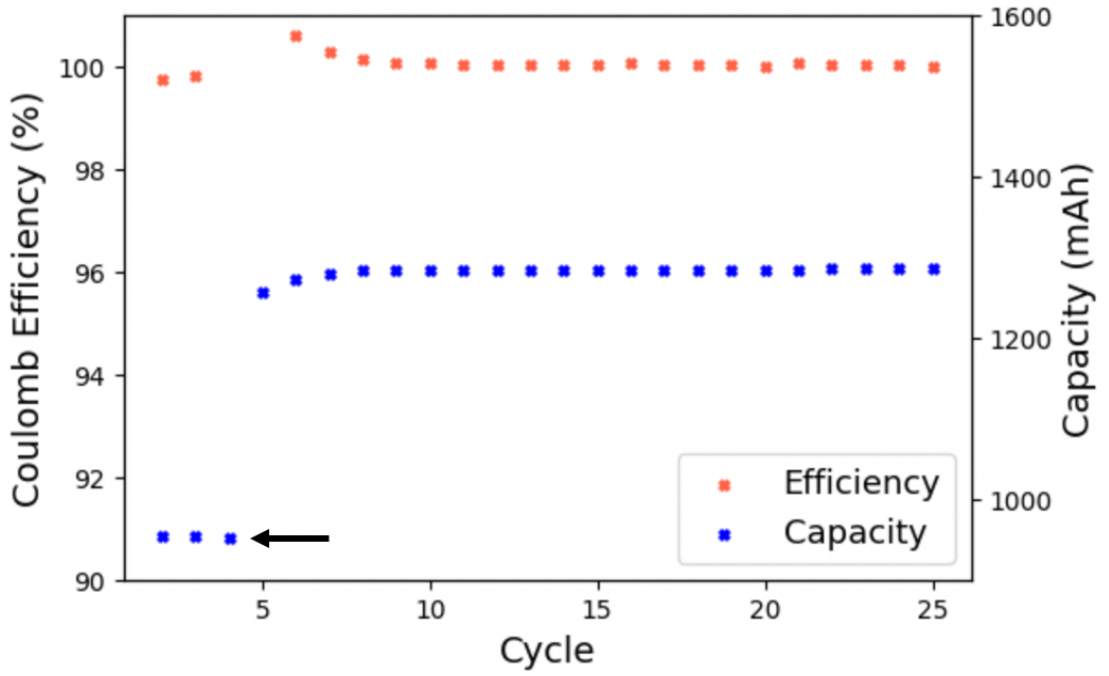

Figure 20: Galvanostatic cycling parameters for a symmetric cell assembled with 50 mL negolyte solution containing 0.0042 moles of PB in boosters (carbon material YP-50F) and 0.8 mol L^{-1} ferricyanide in 1 mol L^{-1} NaCl solution. The system was paired to 200 mL posolyte solution of 0.5 mol L^{-1} ferrocyanide and 0.15 mol L^{-1} ferricyanide in 1 mol L^{-1} NaCl solution. Charging process was CC-CC with ±37.5 mA cm^{-2} (cut off ±0.59 V) with a and ±2.5 mA cm^{-2} (cut off ±0.6 V). The arrow is pointing the capacity of the solution, before adding the boosters.

The boosted tank had 1522 mAh of theoretical storage capacity, of which 450 mAh came from boosters and the rest from the charge-transporting solution. The first program consisted of applying CC(fast)-CC(slow) charge-discharge current densities of ± 37.5 mA cm^{-2} and ± 2.5 mA cm^{-2}.

In the absence of solid boosters, the solution charged to 955 mAh (Figure 20), which represents 89 % of the theoretical capacity of the charge-transporting solution containing 0.8 mol L^{-1} ferricyanide. With and without boosters, the cell exhibited good cycling stability and displayed voltage (VE=78.6 %), energy (EE=78.5 %) and coulombic (CE=100%) efficiencies comparable to previous reports [3, 6]. When adding the boosters, the cell reached a maximum discharge capacity of 1285.0 mAh, indicating that the boosters contributed 330 mAh. This represents 73.3 % of their theoretical capacity which is comparable to the results reported in the literature for similar cells [3, 6]. It should be noted, that Yan et al. reported a volumetric capacity (which also

includes the contribution of the charge-transporting solution) of 95.7 Ah L^{-1} for their booster tanks [3], while Chen et al. reported 61.6 Ah L^{-1} [6]. However, these studies do not specify whether the reported volumetric capacity refers solely to the specific volume of the tank containing the boosters, or if it also includes the solution in other parts of the battery, such as

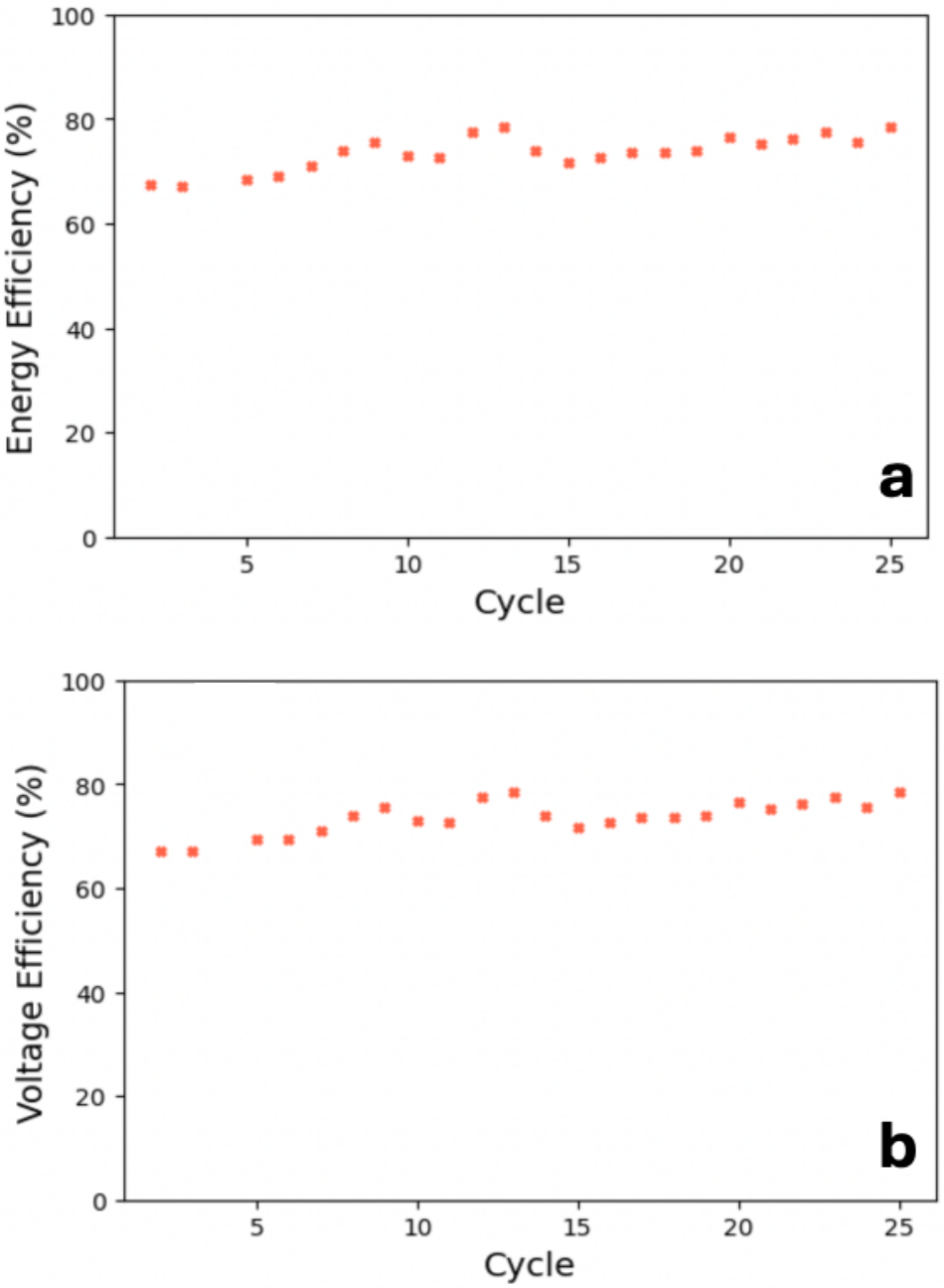

Figure 21: (a) Representation of energy efficiency as a function of number of cell cycles for a symmetric cell assembled with 50 mL negolyte solution containing 0.0042 moles of PB in boosters (carbon material YP-50F) and 0.8 mol L^{-1} ferricyanide in 1 mol L^{-1} NaCl solution. The system was paired to 200 mL posolyte solution of 0.5 mol L^{-1} ferrocyanide and 0.15 mol L^{-1} ferricyanide in 1 mol L^{-1} NaCl solution. Charging process was CC-CC with ±37.5 mA cm^{-2} (cut off ±0.59 V) with a and ±2.5 mA cm^{-2} (cut off ±0.6 V) . (b) Same but for voltage efficiency as a function of number of cell cycles

the connecting pipes. As a consequence, the exact calculation process of the volumetric capacity in these studies remains unclear.

The system used in this study is robust, partly because the goal of this study was not to demonstrate high volumetric capacities, as this was already demonstrated in the literature. While determining the volumetric energy capacity of the space containing the boosters of this study would be interesting, it is also quite challenging.

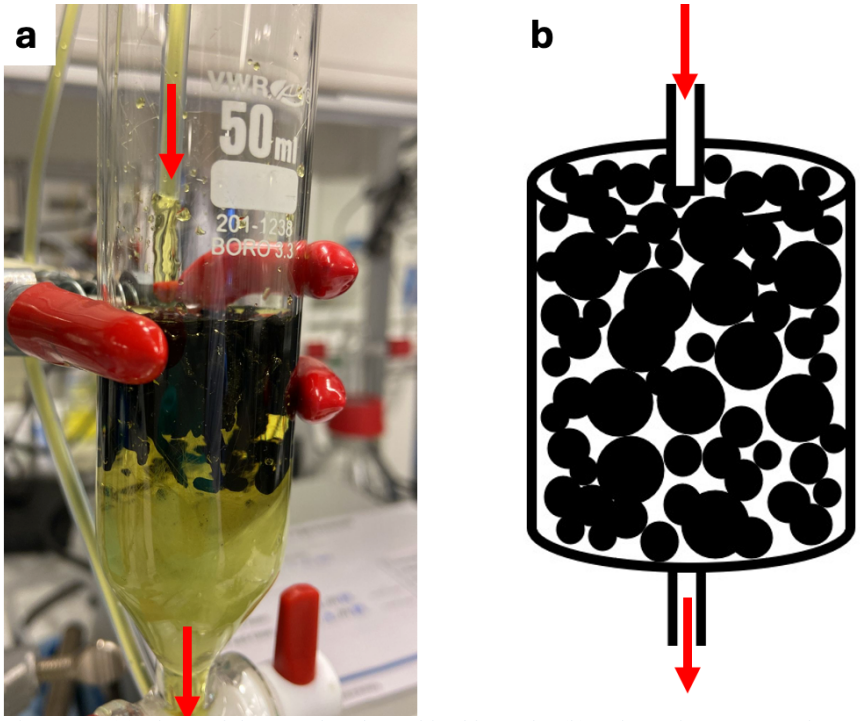

Figure 22: (a) Photo of the actual tank used in this study. (b) Schematic representation of the proposed tank design

Firstly, the negolyte tank design studied here (figure 22a), requires incorporating more solution than boosters (not only in the pipeline), which greatly reduces the tank's energy storage capacity. A promising approach to better estimate the volumetric energy storage capacity would be to calculate it based solely on the volume containing the boosters with a minimal amount of solution. However, this is not possible because the design requires incorporating glass wool to hold the boosters, which creates undefined spaces. To allow for a more reliable volumetric capacity measurement, the design should be modified to create a more compact tank (figure 22b), ensuring that the boosters occupy the entire space. This design would eliminate the excess solution within the tank. In fact, this would result in a significantly higher volumetric capacity value compared to what can be achieved with the current design.

The volume of the tank was also influenced by the air inside the boosters. During the experiments, the space occupied by boosters and dissolution was slowly changing over time, which was initially attributed to the evaporation of the solvent. However, it was also considered possible that air escaped from the boosters while the solution entered them. To try to address this issue, the initial surface level of the tank was market at the start of the experiment, and water was added periodically to maintain the volume as the experiment went on. This was necessary because a decreasing surface level caused some boosters to be unable to come into contact with the solution. However, if a low level was caused by the incorporation of solution into the particles rather than evaporation, there is a possibility that a more diluted solution of unknown concentration of charge-transporting species was used, though it would be close to the initial concentration. Due to these complications, only the utilisation capacity of the boosters was analysed and not the overall volumetric capacity of the tanks.

Due to the exceptional utilisation capacity (73.3 %) demonstrated with the use of big cells, for future work, it is promising to work on the reformulation process of PB solid boosters containing the other carbon materials that gave rise to particles that degrade faster than with carbon material YP-50F.

Based on these results, the carbon material BP2000 could provide greater volumetric capacity than the carbon material YP-50F, if its reformulated boosters achieve significant long-term cycling stability when charged-discharged in a large cell with high concentrations of charge-transporting electrolyte solutions.

Therefore, this cost-effective method for preparing solid boosters is a valuable approach that enables booster production without the need for expensive machinery. It can be applied in future studies to reduce the costs of the system under investigation.

8 Conclusion

Transitioning to a sustainable energy model powered by intermittent sources, such as sun and wind, is urgent due to the impacts of climate change. Flow batteries (FBs) typically store seasonal and stationary energy in posolyte (solution to store positive charge) and negolyte (solution to store negative charge) electrolytes trough external tanks, but their further development requires for tanks with high volumetric energy storage capacity, working with low-cost and earth-abundant electroactive materials.

This thesis introduces a cost-effective method for preparing Prussian blue (PB) solid boosters to externally charge-discharge them in posolyte tanks with $[Fe(CN)6]^{4-/3-}$-based electrolytes as charge-transporting species. The air-stability and four-electron storage capacity of PB electroactive molecules makes this concept highly promising for the development of high volumetric capacity posolyte tanks.

Various formulations of these boosters, incorporating binder, carbon black, KCl, and PB (between 65 to 70%), were developed and their effects on the cycling stability and utilisation capacity of aqueous neutral FBs were analysed. This study found that the choice of carbon materials significantly impacted the performance of the boosters, with the best-performing systems achieving over 1000 charge-discharge cycles and a utilisation capacity of 73.3 %, comparable to those reported in the literature. The selection of boosters with a formulation of 65 % PB, 10 % carbon material YP-50F, 15 % KCl and 10 % binder contributed to improved performance, demonstrating excellent cycling stability.

These findings highlight the potential of low-cost, earth-abundant materials for improving the performance of FBs. Additionally, the results suggest that further optimization of the carbon materials could lead to further advancements in the development of high-performance, cost-effective flow batteries for large-scale energy storage.

References

[1] ”Wind and Solar Intermittency and the Associated Integration Challenges: A Comprehensive Review Including the Status in the Belgian Power System”. Viitattu: 6. maaliskuuta 2025. [Verkossa]. Saatavissa: https://www.mdpi.com/1996-1073/14/9/2630
[2] E. Sánchez-Díez *ym.*, ”Redox flow batteries: Status and perspective towards sustainable stationary energy storage”, *J. Power Sources*, vsk. 481, s. 228804, tammi 2021, doi: 10.1016/j.jpowsour.2020.228804.
[3] S. Yan *ym.*, ”Redox Targeting-based Neutral Aqueous Flow Battery with High Energy Density and Low Cost”, *ChemSusChem*, vsk. 16, nro 19, s. e202300710, 2023, doi: 10.1002/cssc.202300710.
[4] J. Asenjo-Pascual, I. Salmeron-Sanchez, J. R. Avilés-Moreno, P. Mauleón, P. Mazur, ja P. Ocón, ”Understanding Aqueous Organic Redox Flow Batteries: A Guided Experimental Tour from Components Characterization to Final Assembly”, *Batteries*, vsk. 8, nro 10, Art. nro 10, loka 2022, doi: 10.3390/batteries8100193.
[5] V. Singh, S. Kim, J. Kang, ja H. R. Byon, ”Aqueous organic redox flow batteries”, *Nano Res.*, vsk. 12, nro 9, ss. 1988–2001, syys 2019, doi: 10.1007/s12274-019-2355-2.
[6] Y. Chen *ym.*, ”A Stable and High-Capacity Redox Targeting-Based Electrolyte for Aqueous Flow Batteries”, *Joule*, vsk. 3, nro 9, ss. 2255–2267, syys 2019, doi: 10.1016/j.joule.2019.06.007.
[7] I. BALDUCCI, ”Engineering of solid boosters for redox flow batteries”. Viitattu: 26. maaliskuuta 2024. [Verkossa]. Saatavissa: http://etd.adm.unipi.it/
[8] S. Jin *ym.*, ”Near Neutral pH Redox Flow Battery with Low Permeability and Long-Lifetime Phosphonated Viologen Active Species”, *Adv. Energy Mater.*, vsk. 10, nro 20, s. 2000100, 2020, doi: 10.1002/aenm.202000100.
[9] W. Lee, A. Permatasari, ja Y. Kwon, ”Neutral pH aqueous redox flow batteries using an anthraquinone-ferrocyanide redox couple”, *J. Mater. Chem. C*, vsk. 8, nro 17, ss. 5727–5731, 2020, doi: 10.1039/D0TC00640H.
[10] S. Pang, X. Wang, P. Wang, ja Y. Ji, ”Biomimetic Amino Acid Functionalized Phenazine Flow Batteries with Long Lifetime at Near-Neutral pH”, *Angew. Chem. Int. Ed.*, vsk. 60, nro 10, ss. 5289–5298, 2021, doi: 10.1002/anie.202014610.
[11] E. Pedraza *ym.*, ”Unprecedented Aqueous Solubility of TEMPO and its Application as High Capacity Catholyte for Aqueous Organic Redox Flow Batteries”, *Adv. Energy Mater.*, vsk. 13, nro 39, s. 2301929, 2023, doi: 10.1002/aenm.202301929.
[12] M. Qin, G. Wu, K. Zheng, X. Yu, J. Xu, ja J. Cao, ”A highly water-soluble phenoxazine quaternary ammonium compound catholyte for pH-neutral aqueous organic redox flow batteries”, *J. Energy Storage*, vsk. 102, s. 114162, marras 2024, doi: 10.1016/j.est.2024.114162.
[13] X. Fang *ym.*, ”A cooperative degradation pathway for organic phenoxazine catholytes in aqueous redox flow batteries”, *Energy*, vsk. 1, nro 1, s. 100008, maalis 2023, doi: 10.1016/j.nxener.2023.100008.
[14] B. Liu, Y. Li, G. Jia, ja T. Zhao, ”Recent Advances in Redox Flow Batteries Employing Metal Coordination Complexes as Redox-Active Species”, *Electrochem. Energy Rev.*, vsk. 7, nro 1, s. 7, maalis 2024, doi: 10.1007/s41918-023-00205-6.
[15] E. S. Beh, D. De Porcellinis, R. L. Gracia, K. T. Xia, R. G. Gordon, ja M. J. Aziz, ”A Neutral pH Aqueous Organic–Organometallic Redox Flow Battery with Extremely High Capacity Retention”, *ACS Energy Lett.*, vsk. 2, nro 3, ss. 639–644, maalis 2017, doi: 10.1021/acsenergylett.7b00019.
[16] M. Mouselly, H. Alawadhi, ja S. T. Senthilkumar, ”Current status of ferro-/ferricyanide for redox flow batteries”, *Curr. Opin. Electrochem.*, vsk. 48, s. 101581, joulu

2024, doi: 10.1016/j.coelec.2024.101581.
[17] J. Hannonen, A. Tuna, G. Gonzalez, E. Martínez González, ja P. Peljo, ”Investigation of Fe(II) Complexes with 1,10-Phenanthroline and 2,2′;6′,2“-Terpyridine for Aqueous Flow Battery Applications”, *ChemElectroChem*, vsk. 12, nro 5, s. e202400574, 2025, doi: 10.1002/celc.202400574.
[18] ”A Multielectron and High-Potential Spirobifluorene-Based Posolyte for Aqueous Redox Flow Batteries - Pang - 2024 - Angewandte Chemie International Edition - Wiley Online Library”. Viitattu: 13. maaliskuuta 2025. [Verkossa]. Saatavissa: https://onlinelibrary.wiley.com/doi/abs/10.1002/anie.202410226
[19] E. Martínez-González ja P. Peljo, ”Improving the Volumetric Capacity of Gallocyanine Flow Battery by Adding a Molecular Spectator”, *ACS Appl. Energy Mater.*, vsk. 7, nro 17, ss. 7169–7175, syys 2024, doi: 10.1021/acsaem.4c00971.
[20] ”Prussian white analogues as promising cathode for non-aqueous potassium-ion batteries”, *Electrochem. Commun.*, vsk. 77, ss. 54–57, huhti 2017, doi: 10.1016/j.elecom.2017.02.012.
[21] M. Moghaddam, ”Scanning electrochemical microscopy characterization of energy materials”, joulu 2023, Viitattu: 19. heinäkuuta 2024. [Verkossa]. Saatavissa: https://www.utupub.fi/handle/10024/176153
[22] B. Lestriez, S. Bahri, I. Sandu, L. Roué, ja D. Guyomard, ”On the binding mechanism of CMC in Si negative electrodes for Li-ion batteries”, *Electrochem. Commun.*, vsk. 9, nro 12, ss. 2801–2806, joulu 2007, doi: 10.1016/j.elecom.2007.10.001.
[23] C. C. Corporation, ”Calgon Carbon Corporation”, Calgon Carbon Corporation. Viitattu: 10. heinäkuuta 2024. [Verkossa]. Saatavissa: https://www.calgoncarbon.com/search/
[24] ”Search”, Cabot Corporation. Viitattu: 15. heinäkuuta 2024. [Verkossa]. Saatavissa: https://www.cabotcorp.com/search/?query=bp2000
[25] M. Wang *ym.*, ”Investigation of carbon corrosion in polymer electrolyte fuel cells using steam etching”, *Mater. Chem. Phys.*, vsk. 123, nro 2, ss. 761–766, loka 2010, doi: 10.1016/j.matchemphys.2010.05.055.
[26] ”C-NERGY SUPER C65 Conductive Carbon Black”, Nanografi Nano Technology. Viitattu: 21. elokuuta 2024. [Verkossa]. Saatavissa: https://nanografi.com/battery-equipment/c-nergy-super-c65-conductive-carbon-black/
[27] H. Wang *ym.*, ”Redox Flow Batteries: How to Determine Electrochemical Kinetic Parameters”, *ACS Nano*, vsk. 14, nro 3, ss. 2575–2584, maalis 2020, doi: 10.1021/acsnano.0c01281.
[28] H. Yamada, K. Yoshii, M. Asahi, M. Chiku, ja Y. Kitazumi, ”Cyclic Voltammetry Part 1: Fundamentals”, *Electrochemistry*, vsk. 90, nro 10, ss. 102005–102005, 2022, doi: 10.5796/electrochemistry.22-66082.
[29] A. J. Bard ja L. Faulkner, *Electrochemical Methods: Fundamentals and Applications*, 2. p. Wiley, 2000.
[30] J. Savéant, *Elements of Molecular and Biomolecular Electrochemistry: An Electrochemical Approach to Electron Transfer Chemistry*, 1. p. Wiley, 2006. doi: 10.1002/0471758078.
[31] R. M. Dell ja D. A. J. Rand, *Understanding batteries*, 1. p. The Royal Society of Chemistry, 2001.
[32] ”Polarization curve analysis of all-vanadium redox flow batteries | Journal of Applied Electrochemistry”. Viitattu: 4. maaliskuuta 2025. [Verkossa]. Saatavissa: https://link.springer.com/article/10.1007/s10800-011-0335-7
[33] E. Martínez-González, H. G. Laguna, M. Sánchez-Castellanos, S. S. Rozenel, V. M. Ugalde-Saldivar, ja C. Amador-Bedolla, ”Kinetic Properties of Aqueous Organic Redox Flow Battery Anolytes Using the Marcus–Hush Theory”, *ACS Appl. Energy Mater.*, vsk. 3, nro 9,

ss. 8833–8841, syys 2020, doi: 10.1021/acsaem.0c01336.
[34] E. Banguero, A. Correcher, Á. Pérez-Navarro, F. Morant, ja A. Aristizabal, ”A Review on Battery Charging and Discharging Control Strategies: Application to Renewable Energy Systems”, *Energies*, vsk. 11, nro 4, Art. nro 4, huhti 2018, doi: 10.3390/en11041021.
[35] ”Comprehensive Analysis of Critical Issues in All-Vanadium Redox Flow Battery | ACS Sustainable Chemistry & Engineering”. Viitattu: 10. maaliskuuta 2025. [Verkossa]. Saatavissa: https://pubs.acs.org/doi/full/10.1021/acssuschemeng.2c01372
[36] R. Rubio-Presa, L. Lubián, M. Borlaf, E. Ventosa, ja R. Sanz, ”Addressing Practical Use of Viologen-Derivatives in Redox Flow Batteries through Molecular Engineering”, *ACS Mater. Lett.*, vsk. 5, nro 3, ss. 798–802, maalis 2023, doi: 10.1021/acsmaterialslett.2c01105.
[37] ”High Precision Battery Testing System - Landt Instruments”. Viitattu: 6. maaliskuuta 2025. [Verkossa]. Saatavissa: https://landtinst.com/
[38] J. Ostrander, R. Younesi, ja R. Mogensen, ”High Voltage Redox-Meditated Flow Batteries with Prussian Blue Solid Booster”, *Energies*, vsk. 14, nro 22, Art. nro 22, tammi 2021, doi: 10.3390/en14227498.
[39] M. J. Piernas Muñoz ja E. Castillo Martínez, ”Prussian Blue and Its Analogues. Structure, Characterization and Applications”, teoksessa *Prussian Blue Based Batteries*, M. J. Piernas Muñoz ja E. Castillo Martínez, Toim., Cham: Springer International Publishing, 2018, ss. 9–22. doi: 10.1007/978-3-319-91488-6_2.